

ANGULAR DISTRIBUTION OF PROTONS  
FROM  $\text{Ca}^{44}(\text{d},\text{p})\text{Ca}^{45}$  REACTION

---

Warring Crane Cobb  
and  
Douglas Burden Guthe

Library  
U. S. Naval Postgraduate School  
Monterey, California

1-31

PRP	PROTONS
CAL	CALCIUM







ANGULAR DISTRIBUTION OF PROTONS

FROM  $\text{Ca}^{44}(\text{d}, \text{p})\text{Ca}^{45}$  REACTION

8854

COBB

is Cobb  
ival Academy

1955

THESES

0528

Guthe  
ival Academy

Letter on cover:

ANGULAR DISTRIBUTION OF PROTONS  
FROM  $\text{Ca}^{44}(\text{d}, \text{p})\text{Ca}^{45}$  REACTION

Illment of the

Degree of

Harrington Crane Cobb

ENCE

and

Douglas Burden Guthe

OF TECHNOLOGY





# ANGULAR DISTRIBUTION OF PROTONS

FROM  $\text{Ca}^{44}(\text{d},\text{p})\text{Ca}^{45}$  REACTION

by

Warrington Crane Cobb  
Lieutenant, U.S. Navy

and

Douglas Burden Guthe  
Lieutenant, U.S. Navy

Submitted to the Department of Physics on May 23, 1955 in partial fulfillment of the requirements for the degree of Master of Science.

## ABSTRACT

The MIT-ONR electrostatic generator and broad-range spectrograph have been used to study the angular distribution of proton groups from the reaction  $\text{Ca}^{44}(\text{d},\text{p})\text{Ca}^{45}$ . A thin target of  $\text{Ca}^{44}\text{O}$ , backed by Formvar and gold leaf, was bombarded with 7.0-Mev deuterons. The angular distributions for formation of the ground state and ten excited levels of  $\text{Ca}^{45}$  were observed.

The  $\text{Ca}^{44}(\text{d},\text{p})\text{Ca}^{45}$  reaction was observed to proceed predominantly by stripping. The distributions have been compared with the predictions of the Butler stripping theory, in order to determine  $\ell_n$ , the angular momentum of the captured neutron.

The angular momenta and parities for the levels of  $\text{Ca}^{45}$  have been determined as listed below:

$\text{Ca}^{45}$ Level	$\ell_n$	Possible Value of Spin	Parity
Ground State	3	5/2, 7/2	Odd
0.18 Mev	-	-	-
1.43 Mev	1	1/2, 3/2	Odd
1.89 Mev	1	1/2, 3/2	Odd
2.25 Mev	1	1/2, 3/2	Odd
2.40 Mev	0	1/2	Even
2.84 Mev	1 or 2	1/2, 3/2, 5/2	-
2.96 Mev	-	-	-
3.24 Mev	1 or 2	1/2, 3/2, 5/2	-
3.32 Mev	-	-	-
3.42 Mev	1 or 2	1/2, 3/2, 5/2	-



The relative differential cross sections for formation of the various levels have also been calculated.

The conclusions indicated that no single choice of the parameter  $r_0$ , the interaction radius of the Butler theory, resulted in unique determination of  $l_n$  for all the distributions encountered. It has been suggested that the theory of Tobocman may give theoretical predictions to match the experimental results.

Thesis Supervisor: W. W. Buechner

Title: Associate Professor of Physics

The relative efficiency of these systems for detection of the various levels was also calculated.

The observations indicated that as the degree of the noise over the detection system of the system, the relative efficiency of the system was also calculated. It has been suggested that the degree of detection was the same as the degree of the system.

These observations: W. W. D. D.

These observations: Associate Professor of Physics

Department of Physics, University of California, Los Angeles, California

1955

The following observations were made in the course of the investigation. The results of the investigation are given in the following table. The results of the investigation are given in the following table. The results of the investigation are given in the following table.

The following observations were made in the course of the investigation. The results of the investigation are given in the following table. The results of the investigation are given in the following table. The results of the investigation are given in the following table.

The following observations were made in the course of the investigation. The results of the investigation are given in the following table. The results of the investigation are given in the following table. The results of the investigation are given in the following table.

Level	Relative Efficiency	Relative Efficiency	Relative Efficiency
1	0.00	0.00	0.00
2	0.00	0.00	0.00
3	0.00	0.00	0.00
4	0.00	0.00	0.00
5	0.00	0.00	0.00
6	0.00	0.00	0.00
7	0.00	0.00	0.00
8	0.00	0.00	0.00
9	0.00	0.00	0.00
10	0.00	0.00	0.00

## ACKNOWLEDGMENTS

The authors wish to express their appreciation to the entire staff of the High Voltage Laboratory for their friendly assistance and cooperation, without which this work could not have been accomplished.

In particular, we are very grateful to Professor Buschner for supervising this thesis, to Dr. C. K. Bockelman for his constant help and advice, and to Dr. C. P. Browne, Mr. A. Spurdute, Mr. S. Zimmerman, and Mr. R. Sharp for their patient consideration of our many questions.

We should also like to thank Mrs. Grace Rowe for her excellent job of drawing the curves and Misses Sylvia Darrow, Estelle Freedman, and Anna Recupero for their fine job of counting the photographic plates.

Finally, we wish to thank Mrs. Mary E. White for her excellent preparation of the manuscript.



The authors wish to express their appreciation to the staff of the High Voltage Laboratory for their friendly assistance and cooperation, without which this work could not have been accomplished. In particular, we are very grateful to Professor Buchner for supervising this thesis, to Dr. G. E. Hoffman for his constant help and advice, and to Dr. G. E. Brown, Dr. A. E. Bennett, Dr. S. E. Coleman, and Dr. R. E. Smith for their patient consideration of our many questions. We should also like to thank Mr. Grace for his excellent job of drawing the curves and tables, Miss G. E. Coleman, and Miss Bennett for their fine job of counting the photomultiplier plates. Finally, we wish to thank Mr. E. E. Smith for his excellent preparation of the manuscript.

## TABLE OF CONTENTS

	Page number
I. INTRODUCTION	1
II. EXPERIMENTAL PROCEDURE AND APPARATUS	5
III. EXPERIMENTAL RESULTS	7
IV. CONCLUSIONS	20

## TABLES

TABLE I	3
TABLE II	11
TABLE III	13
TABLE IV	18
TABLE V	19

## References

# TABLE OF CONTENTS

Page number

I. INTRODUCTION	1
II. EXPERIMENTAL PROCEDURE AND APPARATUS	2
III. EXPERIMENTAL RESULTS	7
IV. CONCLUSIONS	20
<p>In conclusion, we have shown that the reaction between the</p> <p>hydrogen and oxygen is a first-order reaction with</p> <p>respect to the hydrogen and a half-order reaction with</p> <p>respect to the oxygen. The rate of reaction is independent of the</p> <p>total pressure and is proportional to the square root of the</p> <p>oxygen pressure. The results are in good agreement with the</p> <p>theoretical predictions of the reaction mechanism proposed by</p> <p>the author in his previous paper.</p>	
TABLE I	3
TABLE II	11
TABLE III	13
TABLE IV	18
TABLE V	19

References



## I. INTRODUCTION

The High Voltage Laboratory at the Massachusetts Institute of Technology has been investigating nuclear reactions involving calcium isotopes to provide experimental data upon which predictions of nuclear structure may be made. The calcium isotopes have closed shells of 20 protons.  $\text{Ca}^{40}$  has a closed shell of neutrons; the heavier calcium isotopes are formed by adding neutrons to the  $1f_{7/2}$  shell until the shell is closed at  $\text{Ca}^{48}$ .  $\text{Ca}^{49}$  has one neutron in the  $1f_{5/2}$  shell. Kurath<sup>1</sup> and Edmonds and Flowers<sup>2</sup> have made theoretical studies of the energy-level structure arising from configurations of two, three, and four identical particles in the  $1f_{7/2}$  shell on the basis of the j-j coupling shell model. The latter authors point out that a transition from L-S to j-j coupling is anticipated in the region from  $A = 40$  to 50. This Laboratory has made at least preliminary investigations of the energy levels of  $\text{Ca}^{40,3}$ ,  $\text{Ca}^{41,4}$ ,  $\text{Ca}^{42}$ ,  $\text{Ca}^{43,5}$ ,  $\text{Ca}^{44}$ ,  $\text{Ca}^{45,5}$ ,  $\text{Ca}^{46}$ , and  $\text{Ca}^{49}$ , and of the angular distributions of  $\text{Ca}^{41}$  and  $\text{Ca}^{43,6}$ .

This experiment investigates the angular distribution of protons from the reaction  $\text{Ca}^{44}(d,p)\text{Ca}^{45}$ . The  $\text{Ca}^{45}$  ground state has five neutrons in the  $1f_{7/2}$  shell outside closed shells of 20 neutrons and 20 protons. Problems concerning the states that are formed by re-arrangement of the five neutrons within the  $1f_{7/2}$  shell may be treated the same analytically as the problem of 3 neutrons in the shell, according to the "hole" theory.

# I. INTRODUCTION

The High Voltage Laboratory at the Massachusetts Institute of Technology has been investigating nuclear reaction involving calcium isotopes to provide experimental data upon which prediction of nuclear structure may be made. The calcium isotopes have closed shells of 20 protons.  $Ca^{40}$  has a closed shell of neutrons; the heavier calcium isotopes are formed by adding neutrons to the  $1f_{7/2}$  shell until the shell is closed at  $Ca^{48}$ .  $Ca^{49}$  has one neutron in the  $1f_{7/2}$  shell. Kratz and Flowers<sup>1</sup> and Flowers<sup>2</sup> have made theoretical studies of the energy-level structure arising from configurations of two, three, and four identical particles in the  $1f_{7/2}$  shell on the basis of the  $j-j$  coupling shell model. The latter authors point out that a transition from  $j=3$  to  $j=7/2$  coupling is anticipated in the region from  $A=40$  to  $Ca^{50}$ . This laboratory has made at least preliminary investigations of the energy levels of  $Ca^{40}$ ,  $Ca^{41}$ ,  $Ca^{42}$ ,  $Ca^{43}$ ,  $Ca^{44}$ ,  $Ca^{45}$ ,  $Ca^{46}$ , and  $Ca^{48}$ , and of the angular distributions of  $Ca^{41}$  and  $Ca^{43}$ . This experiment investigates the angular distribution of protons from the reaction  $Ca^{40}(p, Ca^{41})$ . The  $Ca^{40}$  ground state has five neutrons in the  $1f_{7/2}$  shell outside closed shells of 20 protons and 20 neutrons. Problems concerning the states that are formed by re-arrangement of the five neutrons within the  $1f_{7/2}$  shell may be treated the same analytically as the problem of 3 neutrons in the shell, according to the "hole" theory.



The angular distributions of protons from (d,p) reactions are often characterized by pronounced maxima in the forward direction. In order to explain these reactions without postulating high values of angular momentum, the stripping process has been visualized. The Butler<sup>7</sup> theory predicts the angular distributions of protons from these (d,p) reactions in terms of " $\ell_n$ ", the angular momentum of the captured neutron. Butler's calculations indicate that for  $\ell_n = 0$ , the maximum of the angular distribution occurs near  $\theta = 0$ , where  $\theta$  is the angle of observation. As the characteristic value of  $\ell_n$  is increased, the maximum of the angular distribution moves to larger values of  $\theta$ . If the angular momentum and parity of the initial nucleus in the reaction are known, determination of  $\ell_n$  corresponding to the formation of a given level in the final nucleus also determines the parity and possible values of angular momentum for that level. Greater restrictions may be placed on the possible values of angular momentum for the level if  $I = 0$  for the initial nucleus.

In this experiment, the Butler theory has been used to investigate the parities and angular momenta of the ground state and ten excited levels of  $\text{Ca}^{45}$ , listed in Table I.

$\text{Ca}^{45}$  decays by beta emission to  $\text{Sc}^{45}$ . The measured values for  $\text{Sc}^{45}$  of  $I = 7/2^9$  and  $\mu = 4.76^{10*}$  point to a  $f_{7/2}$  ground state because of the position of  $\text{Sc}^{45}$  on the Schmidt diagram. This is as predicted by the extreme single-particle shell model. The  $\beta^-$  decay has a half-life of 163.5 days<sup>11</sup> and an allowed shape on the Kurie plot with  $E_{\text{max}} =$

\*nuclear magnetons.

The angular distribution of neutrons from  $(d,n)$  reactions are often characterized by parameters which in the forward direction in order to explain these reactions without postulating high values of angular momentum, the angular momentum has been calculated. The latter theory predicts the angular distribution of neutrons from  $(d,n)$  reactions in terms of  $l$ , the angular momentum of the captured neutron. The latter's calculation indicates that for  $l = 0$ , the maximum of the angular distribution occurs near  $\theta = 0^\circ$ , where  $\theta$  is the angle of observation. As the characteristic value of  $l$  is increased, the maximum of the angular distribution moves to larger values of  $\theta$ . If the angular momentum and parity of the initial nucleus in the reaction are known, determination of  $l$  corresponding to the formation of a given level in the final nucleus also determines the parity and possible values of angular momentum for that level. Greater restrictions may be placed on the possible values of angular momentum for the level if  $l = 0$  for the initial nucleus.

In this experiment, the latter theory has been used to investigate the positive and angular momentum of the ground state and low excited levels of  $^{10}\text{B}$ , listed in Table I.

The design of the detector is shown in Fig. 1. The measured values for  $^{10}\text{B}$  of  $l = 1$  and  $l = 2$  are  $1.75$  and  $1.50$  respectively. This is as predicted by the reaction of  $d$  on the  $^{10}\text{B}$  target. This is as predicted by the extreme single-particle shell model. The  $l$  theory has a half-life of  $10^{-12}$  sec and an allowed state on the basis plot with  $l = 1$ .

TABLE I  
Excited Levels of  $\text{Ca}^{45}$

0	Ground state
1	0.18 Mev
2	1.43 Mev
3	1.89 Mev
4	2.25 Mev
5	2.40 Mev
6	2.81 Mev
7	2.96 Mev
8	3.24 Mev
9	3.32 Mev
10	3.42 Mev

0.255 Mev<sup>12</sup>. This leads to  $\log ft = 5.9$ . If then the  $\beta^-$  transition is taken to be an allowed one, the result is not in disagreement with the extreme single-particle shell-model prediction of  $f_{7/2}$  for the ground state of  $\text{Ca}^{45}$ . Since  $I = 0$  for the ground state of  $\text{Ca}^{44}$ , the angular distribution of the protons associated with the formation of the ground state of  $\text{Ca}^{45}$  is expected to be characterized by  $\ell_n = 3$ .

The MIT-OMR electrostatic generator and broad-range magnetic spectrograph have been used to study the angular distributions of proton groups resulting from deuteron bombardment of a thin  $\text{Ca}^{44}\text{O}$



TABLE I  
Excited States of  $Ca^{42}$

Ground state	0
0.12 MeV	1
1.13 MeV	2
1.69 MeV	3
2.25 MeV	4
2.70 MeV	5
2.85 MeV	6
2.95 MeV	7
3.24 MeV	8
3.35 MeV	9
3.45 MeV	10

0.25 MeV<sup>12</sup>. This leads to  $J = 2.9$ . If then the  $0^-$  transition is taken to be an allowed one, the results are not in disagreement with the extreme single-particle shell-model prediction of  $2\frac{1}{2}$  for the ground state of  $Ca^{42}$ . Since  $I = 0$  for the ground state of  $Ca^{42}$ , the angular distribution of the electron associated with the formation of the ground state of  $Ca^{42}$  is expected to be characterized by  $L_n = 2$ .

The M $\alpha$ -M $\beta$  electronic monitor and broad-range monitor spectroscopy have been used to study the angular distribution of proton groups resulting from electron bombardment of a thin  $Ca^{42}O$ .

target. The investigation has been carried out at an energy of 7.0 Mev. The proton groups associated with the ground state and the ten excited levels of  $\text{Ca}^{45}$  have been observed at eighteen angles between  $7\frac{1}{2}$  and 120 degrees.

... The investigation has been carried out at an interval of 10 days. The results are given in the following table and the curves of the variation of the level of the water in the reservoir are shown in the figures.

Table 1		Results of the investigation	
No.	Time, days	Level, m	Remarks
1	0	10.0	Start of investigation
2	10	10.5	
3	20	11.0	
4	30	11.5	
5	40	12.0	
6	50	12.5	
7	60	13.0	
8	70	13.5	
9	80	14.0	
10	90	14.5	
11	100	15.0	End of investigation

The results of the investigation show that the level of the water in the reservoir increases steadily over the period of 100 days. The rate of increase is not constant, but the general trend is upwards. The investigation was carried out at an interval of 10 days, and the results are given in the table. The curves of the variation of the level of the water in the reservoir are shown in the figures. The investigation was carried out at an interval of 10 days, and the results are given in the table. The curves of the variation of the level of the water in the reservoir are shown in the figures.



## II. EXPERIMENTAL PROCEDURE AND APPARATUS

Charged particles emerging from the bombarded target were deflected in the magnetic field of the spectrograph and then detected on Eastman NTA 25 $\mu$  photographic plates. The positions of the tracks along the plates determine the radii of curvature of the particles. Calibration of the various distances along the plates was made previously by comparison with the position of alpha-particles from polonium deflected by a known spectrographic field. This procedure has been described elsewhere<sup>16</sup>. The plates were read by counting the number of tracks within each half-millimeter section along the plates. The total length of photographic plate exposed in one run is approximately 76 centimeters. To facilitate plate reading, the plates were covered with thin layers of aluminum foil during exposure on (d,p) runs to prevent charged particles heavier than protons from reaching the emulsion. Detailed descriptions of the MIT-ORNL electrostatic generator and the broad-range spectrograph have been given elsewhere<sup>13-15</sup>.

The target used was prepared by C. N. Braams, presently at the University of Utrecht, while working at this Laboratory. The method was evaporation of CaO onto a thin film of Formvar, backed by gold leaf. The enriched Ca<sup>44</sup> isotope was received in the form of CaCO<sub>3</sub> from the U. S. Atomic Energy Commission, Stable Isotopes Division, Oak Ridge, Tennessee. The calcium content was 97.99 percent Ca<sup>44</sup>; the impurity was mainly Ca<sup>40</sup>.

II. EXPERIMENTAL TECHNIQUE AND RESULTS

Geiger-Müller tubes were used for the detection of the  $\alpha$ -particles in the counting field of the spectrograph and then the tubes on the plates were used for the detection of the  $\beta$ -particles. The position of the tubes along the plates determined the radii of curvature of the particles. Calibration of the various distances along the plates was made by comparison with the position of alpha-particles from a known radioactive source. The plates were used by counting the number of tracks within each half-centimeter section along the plates. The total length of photographic plates exposed in one run is approximately 75 centimeters. To facilitate plate reading, the plates were covered with thin layers of aluminum foil during exposure on (d,p) runs to prevent charged particles from reaching the emulsion. Detailed description of the electrostatic generator and the detection spectrograph have been given elsewhere.<sup>12-15</sup>

The target used was prepared by G. E. Brown, presently at the University of Toronto, while working at this laboratory. The method was evaporation of lead onto a thin film of copper, backed by gold foil. The enriched  $^{64}\text{Zn}$  isotope was separated in the form of  $\text{ZnO}$  from the U. S. Atomic Energy Commission, Stable Isotopes Division, Oak Ridge, Tennessee. The calcium content was 97.99 percent  $^{40}\text{Ca}$ ; the impurity was mainly  $^{44}\text{Ca}$ .

The Butler curves shown in the results were constructed from nomograms prepared by C. R. Lubitz and W. C. Parkinson of the University of Michigan<sup>17</sup>.

The following names were given as the names of the persons who were contacted:



### III. EXPERIMENTAL RESULTS

In order to determine the strong contaminants in the target, a survey was made by bombarding the target with 6-Mev protons and analyzing the elastically scattered proton groups for the masses of the scattering nuclei. The results of this survey are presented in Figure 1. A 400-microcoulomb exposure was used with a spectrograph angle of 120 degrees. The peak for gold is approximately 250-Mev wide at the bottom, thereby obscuring any contaminants of masses between 50 and 197.

A preliminary bombardment of the target with 7-Mev deuterons was made, using an exposure of 500 microcoulombs, and a spectrograph angle of 30 degrees. The resulting proton groups were studied to verify the presence of energy levels of  $\text{Ca}^{45}$ , as found by C. M. Braams. An additional verification was later provided by noting that the energy of proton groups attributed to  $\text{Ca}^{45}$  had the correct dependence upon  $\theta$ .

The preliminary bombardment provided information on the intensities of the various  $\text{Ca}^{45}$  levels. This information was used to determine the exposures required to observe the levels with good statistics.

Experimental data for the angular distribution of  $\text{Ca}^{45}$  were obtained with two bombardment exposures at each angle up to 60 degrees, because of the differences in the intensities of the proton groups

# III. EXPERIMENTAL RESULTS

It was found that the response of the system to a step change in the input is characterized by a delay of approximately 0.5 sec. This delay is due to the time required for the signal to travel from the input to the output. The response of the system to a step change in the input is characterized by a delay of approximately 0.5 sec. This delay is due to the time required for the signal to travel from the input to the output. The response of the system to a step change in the input is characterized by a delay of approximately 0.5 sec. This delay is due to the time required for the signal to travel from the input to the output.

A preliminary experiment of the input with 7-sec duration was made, using an exposure of 500 microsecond, and a resolution of 30 degrees. The resulting traces were studied to verify the response of the system to a step change in the input. The response of the system to a step change in the input is characterized by a delay of approximately 0.5 sec. This delay is due to the time required for the signal to travel from the input to the output.

The resulting traces provided information on the input of the system. This information was used to determine the response of the system to a step change in the input. The response of the system to a step change in the input is characterized by a delay of approximately 0.5 sec. This delay is due to the time required for the signal to travel from the input to the output.

Experimental data for the input distribution of the system was obtained with the following response at each angle up to 30 degrees. The response of the system to a step change in the input is characterized by a delay of approximately 0.5 sec. This delay is due to the time required for the signal to travel from the input to the output.

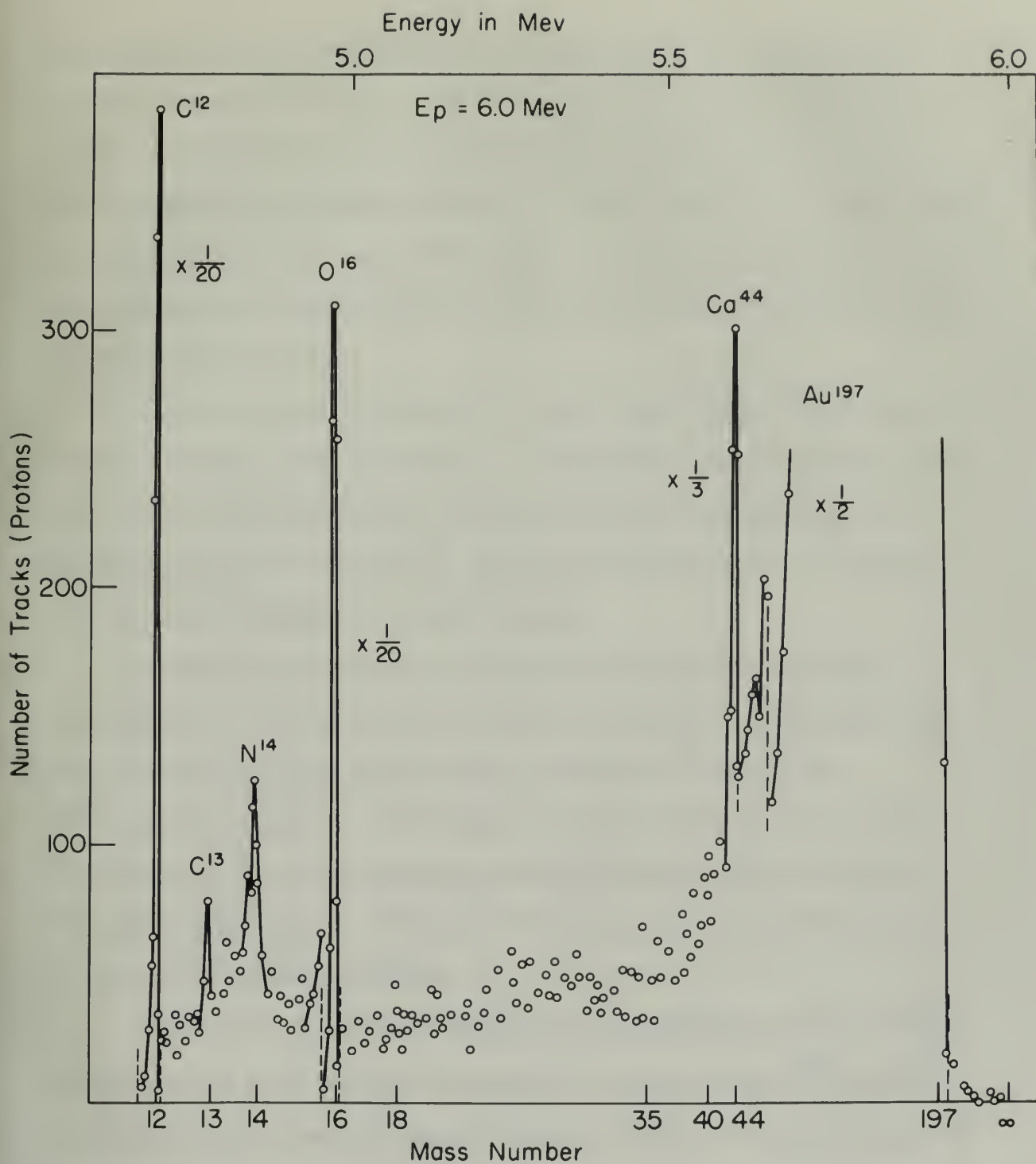


Figure 1





associated with the formation of the various levels. A 3000-micro-coulomb exposure was used to obtain data for the groups corresponding to the ground state and to the 0.18, 2.40, 2.96, and 3.32 Mev levels; a 500-microcoulomb exposure was used to obtain data for the groups corresponding to the 1.43, 1.89, 2.25, 2.84, 3.24, and 3.42 Mev levels. All data obtained at angles from 70 to 120 degrees were obtained with a 500-microcoulomb exposure.

Figure 2 shows representative data obtained with a 500-micro-coulomb exposure. The half-widths of the peaks observed in the experiment varied generally from 1.8 to 3.0 millimeters, corresponding to energy spreads of 16 to 23 kev. The peak width was due to a combination of target thickness and slit opening.

Because of the presence of carbon and oxygen in the target, some levels of  $\text{Ca}^{45}$  could not be observed at certain angles since they were masked by intense proton groups from the  $\text{C}^{12}(\text{d,p})\text{O}^{13}$  and  $\text{O}^{16}(\text{d,p})\text{O}^{17}$  reactions. This situation is made clear in Figure 2 by the intensity of the proton group corresponding to the formation of the ground state of  $\text{C}^{13}$ . Table II tabulates the data missing because of carbon and oxygen reactions.

All levels of  $\text{Ca}^{45}$  were obscured at the 5-degree angle of observation because of an intense background of protons from  $\text{Al}^{27}(\text{d,p})\text{Al}^{28}$  reactions in the aluminum foil covering the plates. At small angles of observation, the number of deuterons scattered into the spectrograph becomes very high.

associated with the formation of the various levels. A 3000-micro-  
coulomb exposure was used to obtain data for the groups corresponding  
to the ground state and to the 0.13, 2.40, 2.96, and 3.32 kev levels;  
a 500-microcoulomb exposure was used to obtain data for the groups corre-  
sponding to the 1.13, 1.59, 2.25, 2.31, 3.21, and 3.42 kev levels. All  
data obtained at angles from 70 to 120 degrees were obtained with a 500-  
microcoulomb exposure.

Figure 2 shows representative data obtained with a 500-micro-  
coulomb exposure. The half-widths of the peaks observed in the experi-  
ment varied generally from 1.8 to 3.0 millielectronvolts, corresponding to  
energy spreads of 16 to 23 kev. The peak width was due to a combina-  
tion of target thickness and slit opening.

Because of the presence of carbon and oxygen in the target,  
some levels of  $Ca^{42}$  could not be observed at certain angles since they  
were masked by intense proton groups from the  $C^{12}(p,\alpha)^{13}C$  and  
 $O^{16}(p,\alpha)^{17}O$  reactions. This situation is made clear in Figure 2 by  
the intensity of the proton group corresponding to the formation of  
the ground state of  $C^{13}$ . Table II tabulates the data missing because  
of carbon and oxygen reactions.

All levels of  $Ca^{42}$  were observed at the 2-degree angle of obser-  
vation because of an intense background of protons from  $Al^{27}(p,\alpha)^{28}Si$   
reactions in the aluminum foil covering the plates. At small angles of  
observation, the number of neutrons scattered into the spectrophotometer  
becomes very high.

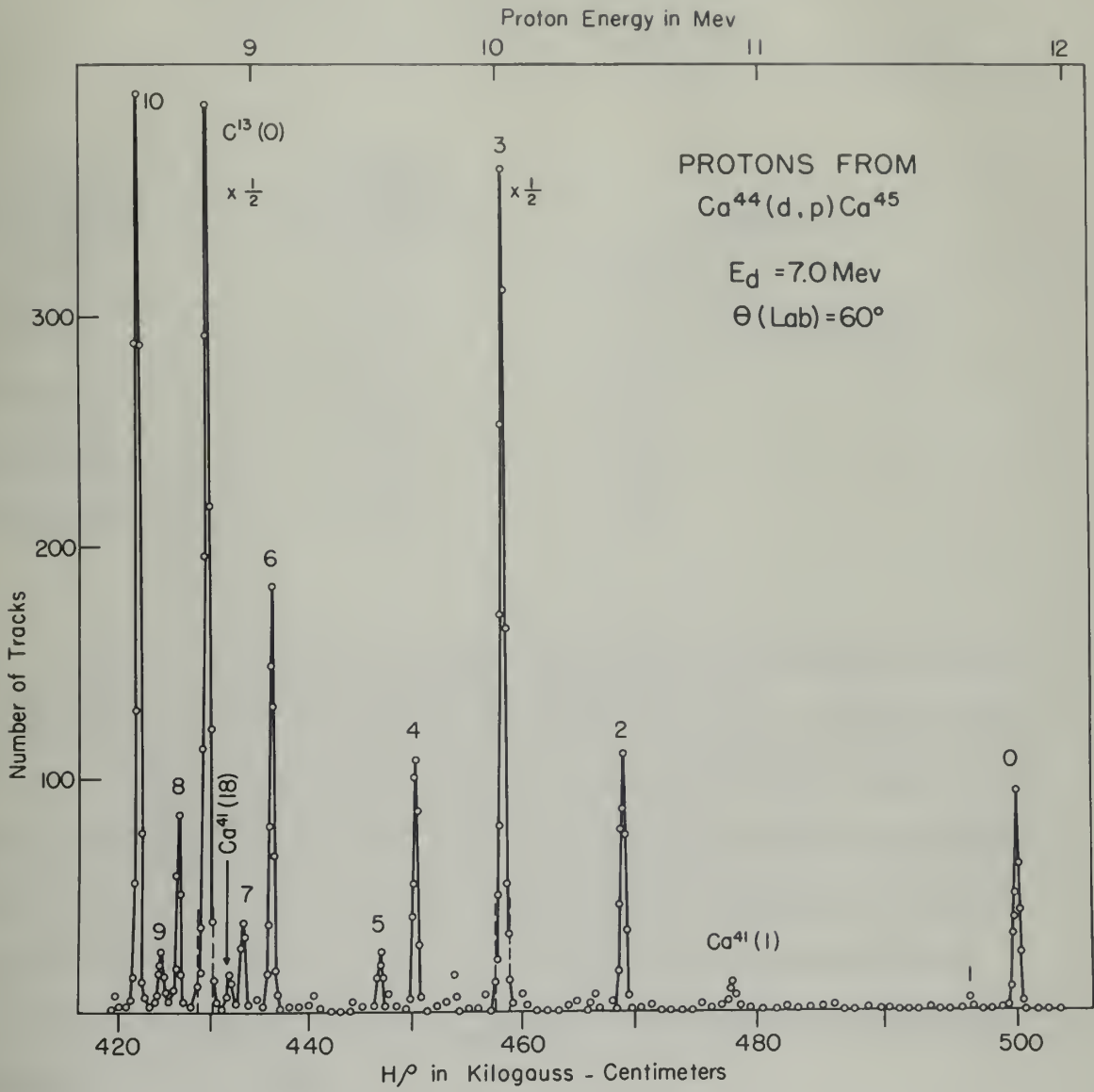


Figure 2





TABLE II

Data Missing Because of Interference from  
 $C^{12}(d,p)C^{13}$  and  $O^{16}(d,p)O^{17}$  Reactions

<u>Obscured Ca<sup>45</sup> Level</u>	<u>Reaction Product Responsible</u>	<u>Angle</u>
3.42 Mev	$O^{17}(O)$	$30^{\circ}, 35^{\circ}$
3.32 Mev	$O^{17}(O)$	$7-1/2^{\circ}, 10^{\circ}, 15^{\circ}, 20^{\circ}$
3.32 Mev	$C^{13}(O)$	$70^{\circ}$
2.96 Mev	$C^{13}(O)$	$50^{\circ}$
2.84 Mev	$C^{13}(O)$	$45^{\circ}$

While observing the angular distribution of protons, the magnetic field of the spectrograph was varied from run to run to cause the ground-state proton group to be observed at the same place on the photographic plates at each angle of observation; this in fact caused the other Ca<sup>45</sup> proton groups to remain almost stationary. This procedure obviated the need for a solid-angle correction caused by a given proton group appearing at different positions as the angle of observation was varied.

To insure that there was no change in the target which might have affected the intensities of the observed proton groups during the successive runs at the various angles, normalizing runs were periodically made at an angle of 60 degrees. The sum of the number of tracks

TABLE II

DATA RELATING TO THE EFFECTS OF TEMPERATURE ON THE  
 $^{13}\text{C}$  AND  $^{15}\text{N}$  NMR SPECTRA

Observed Chemical Shift (ppm)	Assignment of Peaks	Temperature (°C)
3.12 ppm	$^{13}\text{C}(1)$	30°, 35°
3.32 ppm	$^{13}\text{C}(1)$	1-15°, 10°, 15°, 20°
3.32 ppm	$^{13}\text{C}(1)$	10°
2.90 ppm	$^{13}\text{C}(1)$	20°
2.61 ppm	$^{13}\text{C}(1)$	15°

While observing the angular distribution of protons, the  
 ratio field of the spectrometer was varied from 10 to 20  
 the ground-state proton group to be observed at the same place on the  
 photographic plates at each angle of observation; this in fact caused  
 the other  $^{13}\text{C}$  proton groups to remain almost stationary. This two-  
 degree variation was used for a solid-angle correction caused by a  
 given proton group appearing at different positions on the angle of  
 observation was varied.

It is known that there was no change in the magnet which might  
 have affected the intensities of the observed proton groups during the  
 successive runs at the various angles, necessitating runs were periodic-  
 ally made at an angle of 60 degrees. The sum of the number of scans

corresponding to the ground state and to the 1.43- and 2.25-eV levels was mounted for comparison. Normalizing runs were made with an exposure of 500 microcoulombs. Table III outlines the method and results of the normalizing procedure. The results indicate that there was no change in the target.

It was also necessary to insure that a change in the angle of observation,  $\theta$ , did not change the solid angle subtended by the defining slits which are just in front of the photographic plate. To accomplish this, the target was rotated 90 degrees, from  $-45$  degrees from the beam axis to  $+45$  degrees, between runs 5 and 6. As can be seen from the diagram below

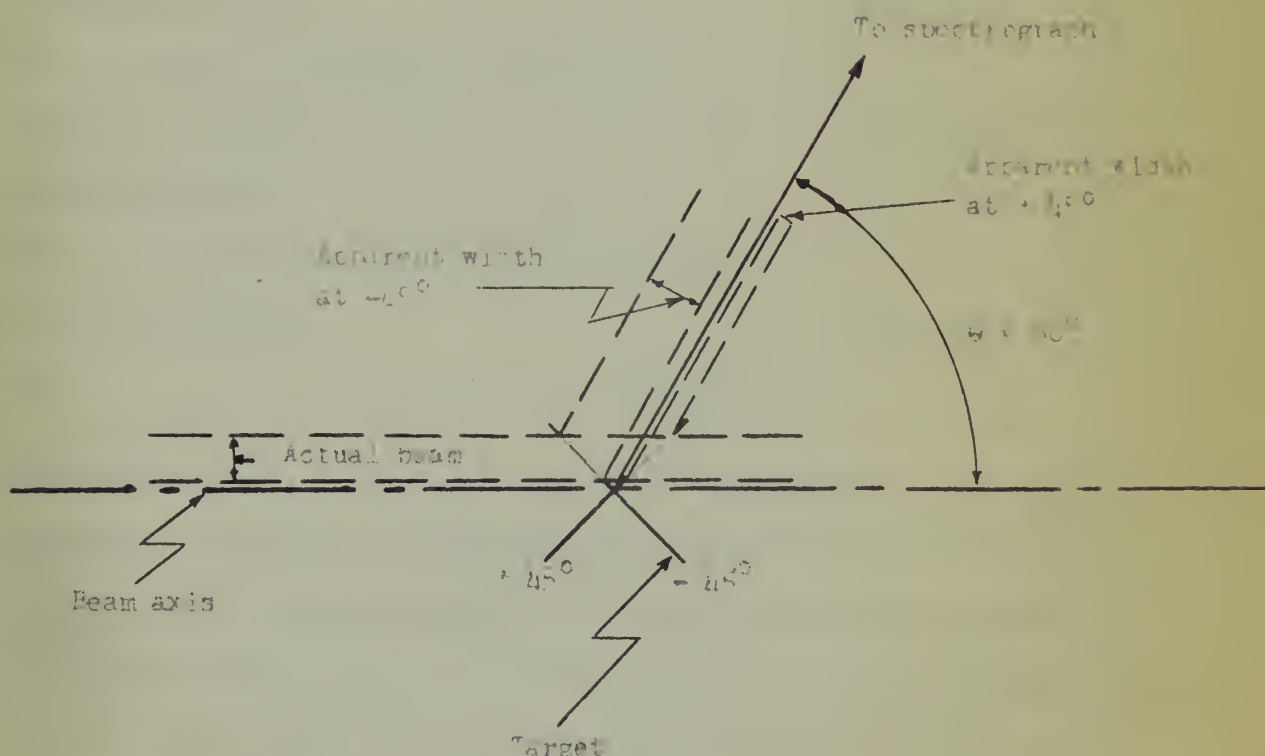






TABLE III

Normalizing Procedure

Order of Runs	Total counts in ground state and 1.43- and 2.25- MeV proton groups + standard deviation
Normalizing run 1	1393 $\pm$ 37
Runs at 50, 40, 30, 20, 10 degrees	
Normalizing run 2	1320 $\pm$ 36
Runs at 60, 55, 45, 35, 25, 15 degrees	
Normalizing run 3	1489 $\pm$ 39
Normalizing run 4	1443 $\pm$ 38
Runs at 7-1/2, 5 degrees	
Normalizing run 5	1472 $\pm$ 38
Normalizing run 6	1437 $\pm$ 38
Runs at 70, 90, 110, 120, 100, 80 degrees	
Normalizing run 7	1416 $\pm$ 38

this rotation did not change the area of the target which was illuminated by the beam even if the beam had been off center; however, it did change the apparent width of the beam spot as viewed from the spectrograph. Since the intensity of the peaks did not change between runs 5 and 6, this indicates that the apparent width of the beam spot did not affect the solid angle observed by the spectrograph.

TABLE III

Normalizing Procedures

Total counts in given state and I.I.- and I.S.- new proton groups $\pm$ standard deviation	Order of runs
$1793 \pm 37$	Normalizing run 1
Runs at 20, 40, 30, 10 degrees	
$1720 \pm 36$	Normalizing run 2
Runs at 60, 25, 15, 35, 25, 15 degrees	
$1678 \pm 36$	Normalizing run 3
$1615 \pm 34$	Normalizing run 4
Runs at 7-1/2, 5 degrees	
$1672 \pm 34$	Normalizing run 5
$1637 \pm 33$	Normalizing run 6
Runs at 70, 90, 110, 130, 150, 80 degrees	
$1616 \pm 33$	Normalizing run 7

This rotation did not change the size of the target which was 11mm-  
 noted for the beam even if the beam had been off center; however, it  
 did change the apparent width of the beam spot as viewed from the spec-  
 trograph. Since the intensity of the beam did not change between runs  
 2 and 6, this indicates that the apparent width of the beam spot did  
 not affect the solid angle observed by the spectrograph.

Figures 3 through 21 show the experimental angular distributions plotted with the calculated Butler curves. The errors shown represent the statistical counting errors only, based on a standard deviation. The spectrograph accepted particles with angles  $1/4$  degree either side of the nominal angle  $\theta$ .

The Butler curves, as plotted, are not corrected for the difference between  $\theta_{lab}$  and  $\theta_{C.M.}$  or for the difference between the solid angle in laboratory and solid angle in center-of-mass coordinates.

Using the formulas,

$$\tan \theta_{lab} = \frac{\sin \theta_{C.M.}}{\gamma + \cos \theta_{C.M.}}$$

$$m_1 \triangleq M_{\text{deuteron}}$$

$$m_2 \triangleq M_{Ca44}$$

$$m_3 \triangleq M_{\text{proton}}$$

$$\gamma = \sqrt{\frac{m_1 m_3}{m_2 m_1} \frac{E_d \text{ in C. M.}}{E_d \text{ in C.M.} + Q}}$$

$$m_4 \triangleq M_{Ca45}$$

$$E_d \text{ in C.M.} = \frac{m_2}{m_1 + m_2} E_{d,lab}$$

$$\text{and } \frac{d\Omega_{C.M.}}{d\Omega_{lab}} = \cos(\theta_{C.M.} - \theta_{lab}) \left( \frac{\sin \theta_{lab}}{\sin \theta_{C.M.}} \right)^2,$$

one gets the following results for the tenth excited level at 3.42 Mev:

$\theta_{C.M.}$	$\theta_{lab}$	$\Delta \theta$	$\frac{d\Omega_{C.M.}}{d\Omega_{lab}}$
$10^\circ$	$9^\circ 43'$	$17'$	$0.944$
$50^\circ$	$48^\circ 48'$	$1^\circ 12'$	$0.967$





The corrections for this state are largest, since it has the lowest  $Q$ -value. Over the range of interest,  $\theta = 10^\circ$  to  $50^\circ$ , where the maxima occur, both corrections are smaller than the error introduced by the nomogram.

One undetermined parameter in the calculation of the angular distribution in the Butler theory is the interaction radius,  $r_0$ .

Huby<sup>18</sup> has stated that Gamov's<sup>19</sup> formula

$$r_0 = (1.22 A^{1/3} + 1.7) \times 10^{-13} \text{ cm.}$$

gives a radius which will normally support unique determinations of  $\ell_n$ . This formula gives  $r_0 = 6.0 \times 10^{-13}$  cm. for  $\text{Ca}^{45}$ . The results of this experiment indicate that no one value for  $r_0$  will lead to unique values of  $\ell_n$ ; therefore, the experimental data have been presented with Butler curves employing  $r_0 = 6.0$  and  $7.0$  on Figures 3 through 21.

The experimental data on Figures 3 through 21 have been interpreted as follows:

Figures 3 and 4 illustrate the ground-state distribution. It is characterized by  $\ell_n = 3$ ;  $r_0 = 7.0$  provides the best fit.

The 0.18-Mev level is not illustrated. The state was detected at the indicated energy but was observed with such low intensity that the angular distribution could not be determined.

Figures 5 and 6 illustrate the 1.43-Mev level distribution. It is characterized by  $\ell_n = 1$ ;  $r_0 = 6.0$  provides the best fit.



The correction for this effect was ignored, since it was the  
lowest deviation. Over the range of interest,  $\alpha = 10^\circ$  to  $20^\circ$ , where the  
correction is small, both corrections are smaller than the error introduced  
by the hypothesis.

The calculated curves in the neighborhood of the origin  
distribution in the latter theory is the Gaussian series,  $\chi^2$ .

$$f_0 = (1.22 A)^{1/2} + 1.7 \times 10^{-13} \text{ cm.}$$

gives a value which will remain constant under consideration of  
 $\chi^2$ . This formula gives  $\chi^2 = 0.0 \times 10^{-13}$  cm. for  $\alpha = 10^\circ$ . The re-  
sult of this experiment indicates that no value for  $\chi^2$  will lead  
to other values of  $\chi^2$ . Therefore, the experimental data have been  
presented with curves corresponding to  $\chi^2 = 0.0$  and  $7.0$  on figures 3  
through 5.

The experimental data on figures 3 through 5 have been inter-  
preted as follows:

Figures 3 and 4 illustrate the ground-state distribution. It  
is characterized by  $\chi^2 = 0$  to  $7.0$  provides the best fit.  
The 0.15-kev level is not illustrated. The curve was reported  
at the indicated energy but was observed with such low intensity that  
the regular distribution could not be determined.

Figures 5 and 6 illustrate the 1.1-kev level distribution. It  
is characterized by  $\chi^2 = 0$  to  $7.0$  provides the best fit.

Figures 7 and 8 illustrate the 1.89-Mev level distribution. It is probably an  $\ell_n = 1$  distribution;  $r_0 = 6.0$  provides the best fit.

Figures 9 and 10 illustrate the 2.25-Mev level distribution. It is characterized by  $\ell_n = 1$ ;  $r_0 = 6.0$  provides the best fit.

Figures 11 and 12 illustrate the 2.40-Mev level distribution. It is characterized by  $\ell_n = 0$ .

Figures 13 and 14 illustrate the 2.94-Mev level distribution. It is probably an  $\ell_n = 2$  distribution; however, the fit is somewhat ambiguous at both values of  $r_0$ .

Figure 15 illustrates the 2.96-Mev level distribution. No determination of  $\ell_n$  is possible. The asymmetry about 90 degrees suggests that stripping action takes place in the formation of this level, but it does not appear to be the characteristic "Butler" type.

Figures 16 and 17 illustrate the 3.24-Mev level distribution. It is probably an  $\ell_n = 2$  distribution; the fit is ambiguous with  $r_0 = 6.0$ .

Figures 18 and 19 illustrate the 3.32-Mev level distribution. The data do not justify the assignment of  $\ell_n$ . There is doubt whether the characteristic "Butler" type stripping takes place in the formation of this level. For comparison only,  $\ell_n = 3$  curves are shown.

Figures 20 and 21 illustrate the 3.42-Mev level distribution. It is probably an  $\ell_n = 2$  distribution, but the fit is poor. The assignment of  $\ell_n$  might have been more definite had the level not been obscured at 30 and 35 degrees.

Figures 7 and 8 illustrate the 1.5% level distribution. It is probably an  $L_n = 1$  distribution;  $r_0 = 0.0$  provides the best fit.

Figures 9 and 10 illustrate the 2.5% level distribution. It is characterized by  $L_n = 1$ ;  $r_0 = 0.0$  provides the best fit.

Figures 11 and 12 illustrate the 5.0% level distribution. It is characterized by  $L_n = 0$ .

Figures 13 and 14 illustrate the 2.5% level distribution. It is probably an  $L_n = 2$  distribution; however, the fit is somewhat ambiguous at both values of  $r_0$ .

Figure 15 illustrates the 2.5% level distribution. No determination of  $L_n$  is possible. The assignment about 20 degrees suggests that striking action takes place in the formation of this level, but it does not appear to be the characteristic "baker" type.

Figures 16 and 17 illustrate the 3.5% level distribution. It is probably an  $L_n = 2$  distribution; the fit is ambiguous with  $r_0 = 0.0$ .

Figures 18 and 19 illustrate the 3.5% level distribution. The data do not justify the assignment of  $L_n$ . There is doubt whether the characteristic "baker" type striking action takes place in the formation of this level. For comparison only,  $L_n = 3$  curves are shown.

Figures 20 and 21 illustrate the 3.5% level distribution. It is probably an  $L_n = 2$  distribution, but the fit is poor. The assignment of  $L_n$  might have been more definite had the level not been observed at 30 and 35 degrees.



Table IV tabulates the assignments of spin and parity to the states of  $\text{Ca}^{45}$  made as a result of the conclusions drawn above.

The intensity of the peaks from the various levels at their maxima was compared with the intensity of the ground state at  $\theta = 40$  degrees, in order to calculate the relative differential cross sections. These relative cross sections and the angle at which they were compared are tabulated in Table IV. In these calculations, solid-angle corrections were used to correct for the different locations of the proton groups. The solid-angle corrections were taken from a curve prepared by S. F. Zimmerman, Jr, of this laboratory.

An attempt was made to determine absolute cross sections by comparison of the observed intensities of the (d,p) reactions with the intensity of Rutherford scattering of 5.0-Mev alpha-particles by  $\text{Ca}^{44}$ . This proved not to be possible with the gold-backed targets available, because the peak of the alpha-particles scattered by gold was wide enough to obscure the  $\text{Ca}^{44}$  peak.

The Butler curves, as calculated, represent only the angular distributions. A multiplying factor was required to apply to each calculated curve in order to match the maximum to the maximum of the experimental data. The factor for the 2.40-Mev level was obtained by matching the Butler curve to the experimental data at  $\theta = 10$  degrees. The factors are listed in Table V. The factors are normalized so as to be equal to unity for the  $\rho_n = 1$ ,  $r_0 = 6.0$ , Butler curve. A solid-angle correction was made.

Table IV tabulates the calculated values of  $\sigma_{\text{rel}}$  and  $\sigma_{\text{abs}}$  for the  
 values of  $\sigma_{\text{rel}}$  and  $\sigma_{\text{abs}}$  of the calculated values of  $\sigma_{\text{rel}}$  and  $\sigma_{\text{abs}}$ .  
 The intensity of the peaks from the various levels of the  
 nucleus was compared with the intensity of the ground state of  
 $\theta = 10$  degrees, in order to calculate the relative differential cross  
 sections. These relative cross sections and the angle at which they  
 were measured are tabulated in Table IV. In these calculations,  
 solid-angle corrections were used to correct for the different loss-  
 flows of the proton groups. The solid-angle corrections were taken  
 from a curve measured by S. V. Zaslavskiy, et al. of this laboratory.  
 In attempt was made to determine absolute cross sections by  
 comparison of the observed intensities of the  $(\alpha, \gamma)$  reactions with the  
 intensity of  $\alpha$ -particle scattering of 5.0-MeV  $\alpha$ -particles by  $\text{Ca}^{40}$ .  
 This proved not to be possible with the gold-coated targets available,  
 because the peak of the  $\alpha$ -particle scattering by gold was wide  
 enough to obscure the  $\text{Ca}^{40}$  peak.  
 The  $\alpha$ -particle curves, as calculated, represent only the angular  
 distribution. A multiplying factor was required to apply to each  
 calculated curve in order to match the curves to the maxima of the  
 experimental data. The factor for the 5.0-MeV level was obtained by  
 matching the  $\alpha$ -particle curve to the experimental data at  $\theta = 10$  degrees.  
 The factors are listed in Table V. The factors are normalized so as  
 to be equal to unity for the  $\alpha$  - 1,  $\gamma$  - 0.0,  $\alpha$  - 0.0,  $\alpha$  - 0.0  
 angle correction was made.



TABLE IV

## Tabulation of Results

Differential  
Cross Section  
Relative to  
Ground State  
at 400  
± 5 percent.

Peak	Q (MeV)	Excita- tion (MeV)	$\ell$ n	Parity	Possible Values of Spin		$\theta$
0	5.19	0	3	Odd	5/2, 7/2	1.0	40°
1	5.01	0.18	-	-	-	≤ 0.05	all
2	3.76	1.43	1	Odd	1/2, 3/2	1.95	20°
3	3.30	1.89	1	Odd	1/2, 3/2	11.3	20°
4	2.94	2.25	1	Odd	1/2, 3/2	1.87	15°
5	2.79	2.40	0	Even	1/2	1.83	7-1/2°
6	2.35	2.84	1 or 2	-	1/2, 3/2, 5/2	2.06	20°
7	2.23	2.96	-	-	-	0.18	35°
8	1.95	3.24	1 or 2	-	1/2, 3/2, 5/2	0.991	20°
9	1.87	3.32	-	-	-	0.180	40°
10	1.77	3.42	1 or 2	-	1/2, 3/2, 5/2	4.17	15°

Task	E (VWA)	Q	Weight	Weight of section	Relative to mean section	Efficiency	Q
10	17.1	24.5	102 S	-	1/5, 3/5, 2/5	1.11	120
2	18.1	24.5	-	-	-	0.770	100
3	18.1	24.5	102 S	-	1/5, 3/5, 2/5	0.701	500
4	18.5	24.5	-	-	-	0.712	320
5	18.2	24.5	102 S	-	1/5, 3/5, 2/5	0.506	500
6	18.5	24.5	0	1000	1/5	1.11	1-1/5
7	18.5	24.5	1	1000	1/5, 3/5	1.11	100
8	18.0	24.5	1	1000	1/5, 3/5	1.11	500
9	18.0	24.5	1	1000	1/5, 3/5	1.11	500
11	18.2	24.5	-	-	-	20.02	100
12	18.2	24.5	3	1000	2/5, 1/5	1.0	100

VI. 1947

Relative to section

TABLE V

<u>Ca<sup>45</sup> Level</u>	<u>Butler Curve</u>		<u>Relative Multiplying Factor</u>
	<u><math>\ell</math></u>	<u><math>n</math></u>	
Ground State	3	6.0	2.59
"	3	7.0	1.47
1.43-Mev Level	1	6.0	1.00
"	1	7.0	0.71
1.89-Mev Level	1	6.0	5.34
"	1	7.0	4.01
"	2	7.0	7.18
2.25-Mev Level	1	6.0	0.78
"	1	7.0	0.56
2.40-Mev Level	0	6.0	0.76
"	0	7.0	0.70
2.84-Mev Level	1	6.0	0.78
"	2	6.0	1.56
"	1	7.0	0.56
"	2	7.0	1.02
3.24-Mev Level	1	6.0	0.33
"	2	6.0	0.71
"	2	7.0	0.46
3.32-Mev Level	3	6.0	0.27
"	3	7.0	0.17
3.42-Mev Level	1	6.0	1.34
"	2	6.0	2.83
"	2	7.0	1.93

TABLE 7

Station Name	Station Number	Station Elevation
Station 1	1	1.00
Station 2	2	1.00
Station 3	3	1.00
Station 4	4	1.00
Station 5	5	1.00
Station 6	6	1.00
Station 7	7	1.00
Station 8	8	1.00
Station 9	9	1.00
Station 10	10	1.00
Station 11	11	1.00
Station 12	12	1.00
Station 13	13	1.00
Station 14	14	1.00
Station 15	15	1.00
Station 16	16	1.00
Station 17	17	1.00
Station 18	18	1.00
Station 19	19	1.00
Station 20	20	1.00
Station 21	21	1.00
Station 22	22	1.00
Station 23	23	1.00
Station 24	24	1.00
Station 25	25	1.00
Station 26	26	1.00
Station 27	27	1.00
Station 28	28	1.00
Station 29	29	1.00
Station 30	30	1.00



#### IV. CONCLUSIONS

Agreement with the Butler theory seems adequate to assign values of  $\ell_n$  with assurance to the distributions for the ground state and first five excited levels, with the exception of the first excited state. Assignment of  $\ell_n$  to the distributions for the next five excited states is somewhat dubious.

It is emphasized that no unique value of  $r_0$  results in positive determinations of  $\ell_n$ . It is further noted that those states assigned  $\ell_n = 1$  were best fitted by  $r_0 = 6.0$ , whereas the ground state, assigned  $\ell_n = 3$ , and the 2.8h- and 3.2h-Mev levels, with probable values of  $\ell_n = 2$ , are best fit by a higher  $r_0$ .

It is concluded that the Butler theory is not complete enough in all cases to make unambiguous assignments of  $\ell_n$ . It appears that a more elaborate treatment is necessary.

Tobocman<sup>20</sup> has developed an extension of the Butler theory by considering the effect of Coulomb and nuclear interactions. The Coulomb effect would seem to be small, since the bombarding energy of 6.7 Mev in center-of-mass coordinates was above the Coulomb barrier of 5.6 Mev. However, only a slight shift of the maxima of the theoretical curves is required for good agreement with experiment.

According to Tobocman, the Coulomb interaction tends to move the maxima to larger angles and broaden the peaks and to fill the valleys between the primary and secondary maxima. However, the nuclear interaction tends to displace the peaks toward smaller angles



#### IV. CONCLUSIONS

Agreement with the Butler theory seems adequate to explain values of  $L$ , with assurance to the distribution for the ground state and first five excited levels, with the exception of the first excited state. Assignment of  $L$  to the distribution for the next five excited states is somewhat dubious.

It is emphasized that no unique value of  $r_0$  results in possible determinations of  $L$ . It is further noted that these states assigned  $L = 1$  were best fitted by  $r_0 = 6.0$ , whereas the ground state, assigned  $L = 3$ , and the 2.5- and 3.5-levels, with probable values of  $L = 2$ , are best fit by a higher  $r_0$ .

It is concluded that the Butler theory is not complete enough in all cases to make unambiguous assignments of  $L$ . It appears that a more elaborate treatment is necessary.

So Tobocean<sup>50</sup> has developed an extension of the Butler theory by considering the effect of Coulomb and nuclear interactions. The Coulomb effect would seem to be small, since the binding energy of 6.7 Mev in center-of-mass coordinates was above the Coulomb barrier of 5.6 Mev. However, only a slight shift of the nuclei of the two- $\alpha$  system is required for good agreement with experiment.

According to Tobocean, the Coulomb interaction tends to move the nuclei to larger angles and broaden the beam and to fill the valleys between the primary and secondary minima. However, the nuclear interaction tends to displace the nuclei toward smaller angles

and to make them less broad. A machine calculation is required to find the predicted position of the primary maxima according to the theory of Toboocman<sup>21</sup>.

The data of this experiment make available for study the angular distributions of the ground state and six excited levels which appear to have almost pure stripping-type distributions. It is believed that the additional work necessary to make a machine calculation would be warranted in order to determine to what degree Toboocman's theory agrees with experiment.

and to make them less broad. A similar calculation is required to find the probability of the primary maxima according to the

theory of Laplace.

The data of this experiment are available for study the angular distribution of the primary state and six excited levels which appear to have almost pure standing-wave distributions. It is believed that the  $n=1/2$  level is necessary to make a similar calculation would be warranted in order to determine in what degree

Laplace's theory agrees with experiment.

It is concluded that the data of this experiment are in good agreement with the theory of Laplace. The data of this experiment are in good agreement with the theory of Laplace. The data of this experiment are in good agreement with the theory of Laplace.

The data of this experiment are in good agreement with the theory of Laplace. The data of this experiment are in good agreement with the theory of Laplace. The data of this experiment are in good agreement with the theory of Laplace.

The data of this experiment are in good agreement with the theory of Laplace. The data of this experiment are in good agreement with the theory of Laplace. The data of this experiment are in good agreement with the theory of Laplace.

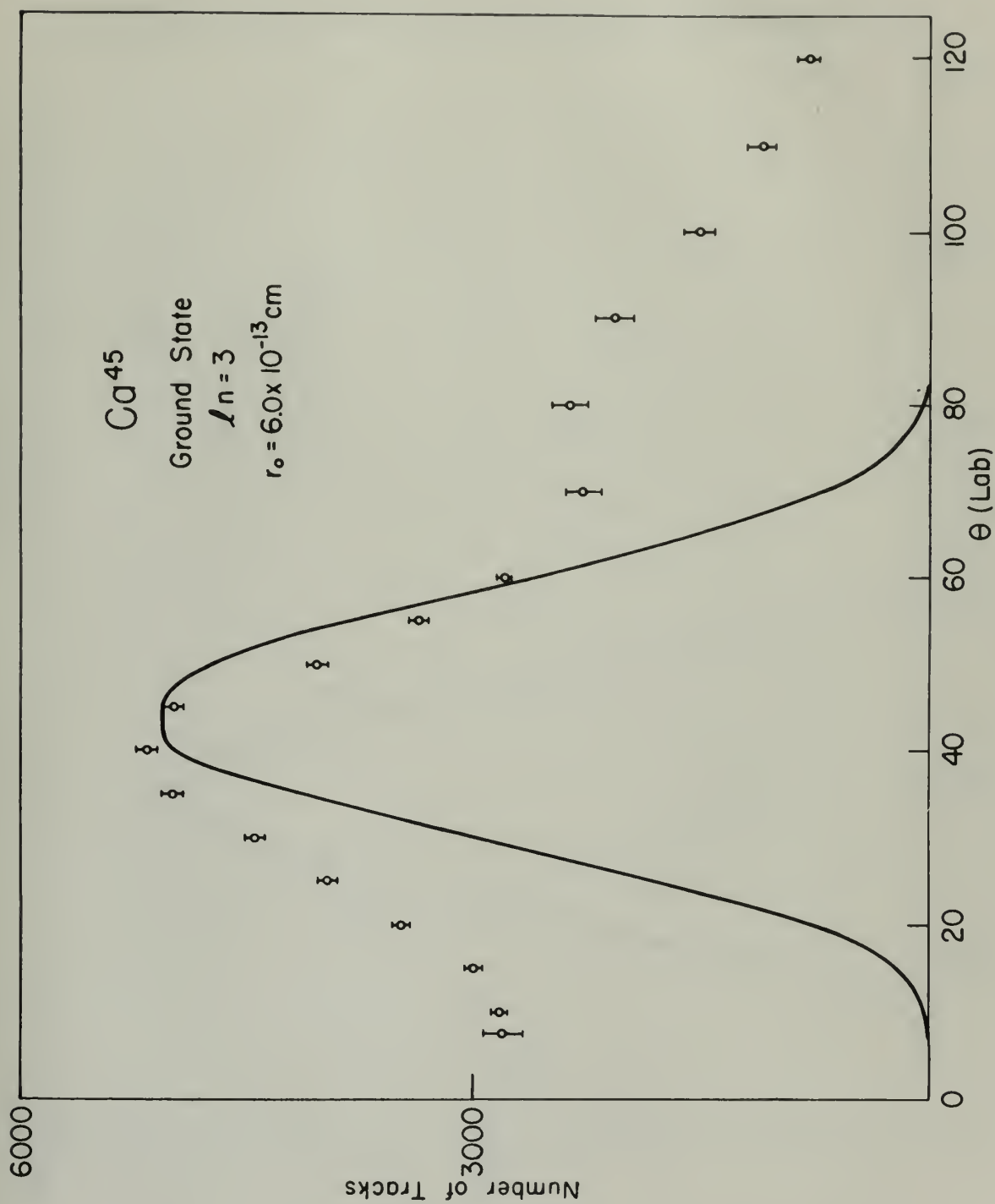


Figure 3





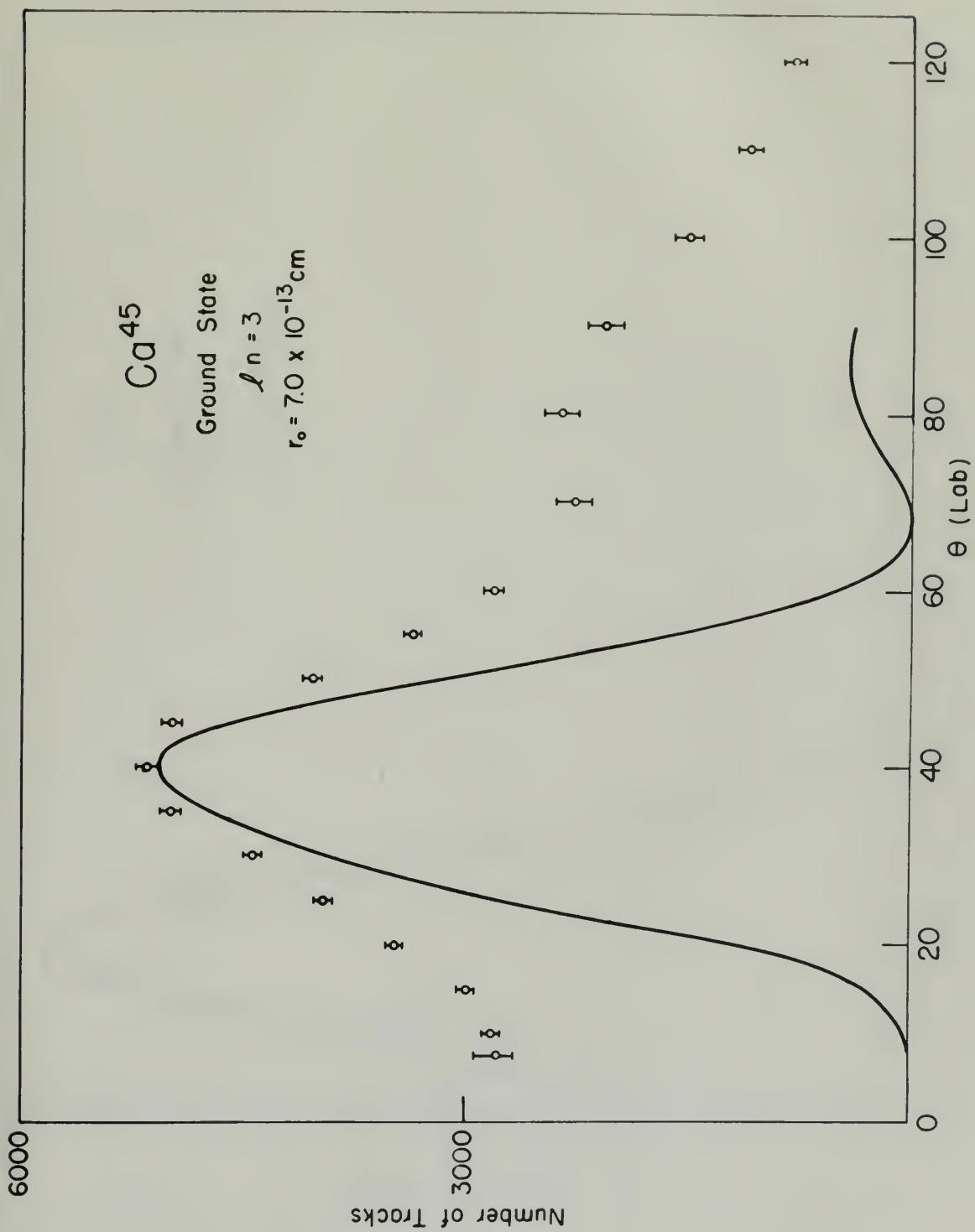


Figure 4



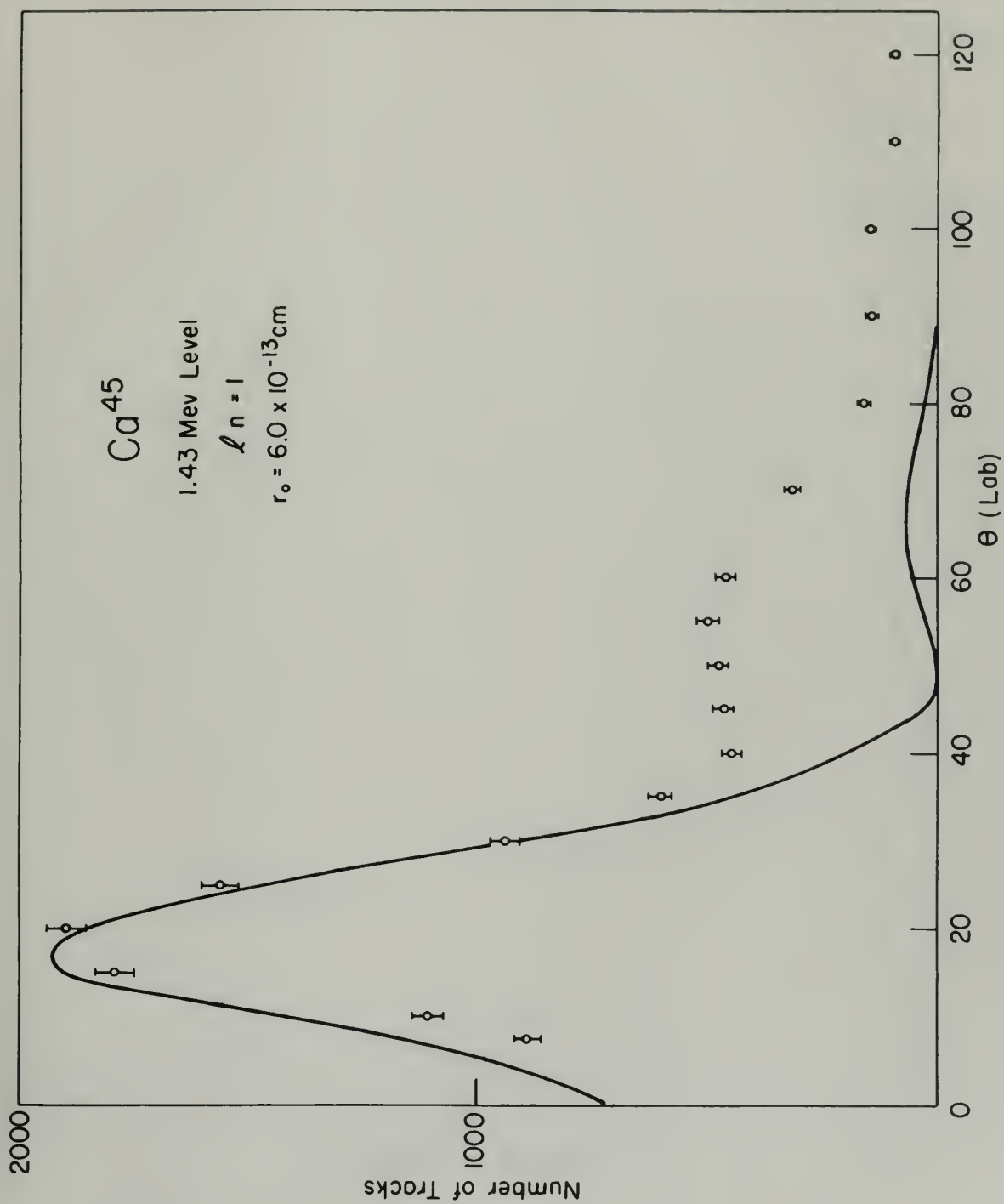


Figure 5





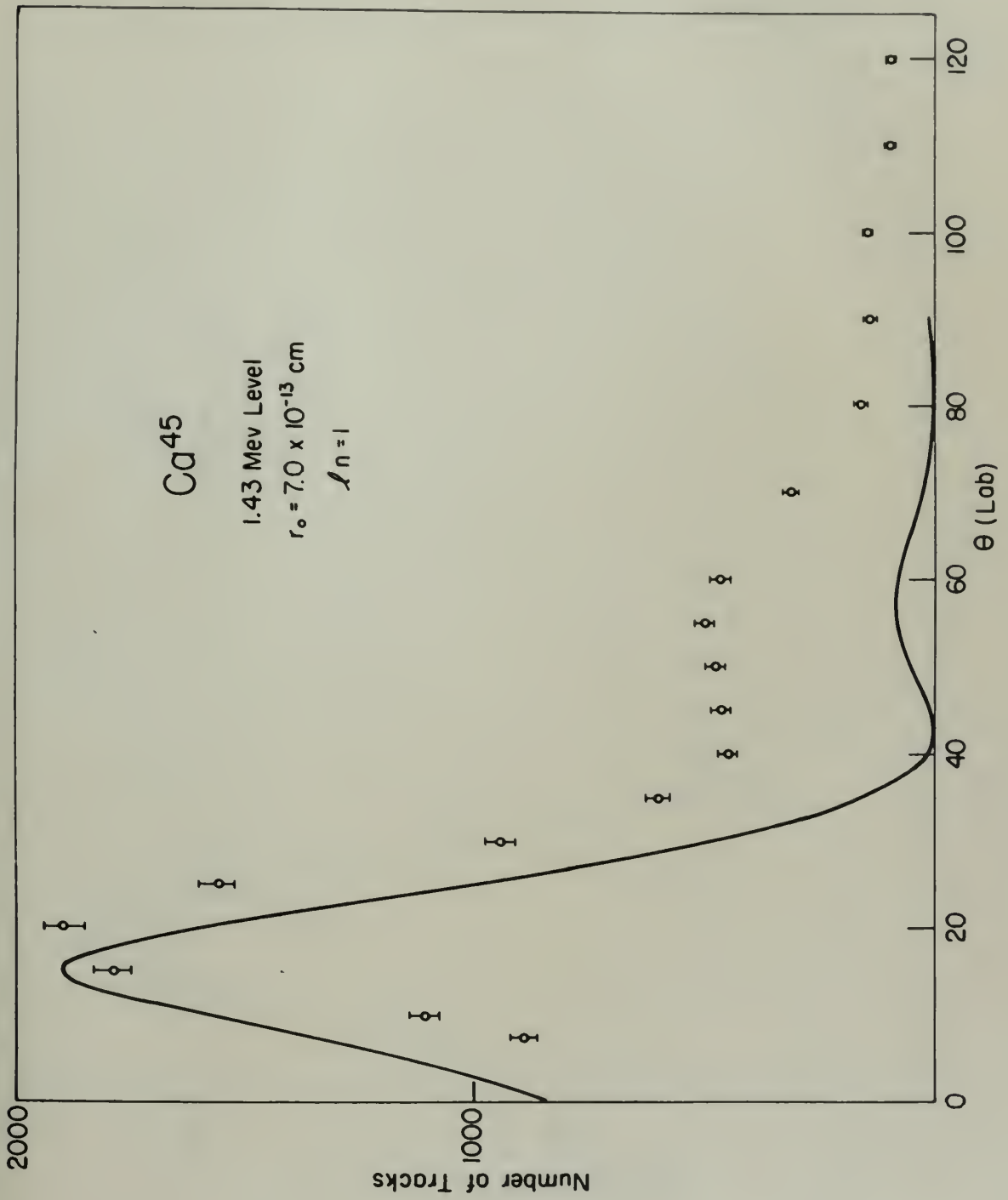


Figure 6



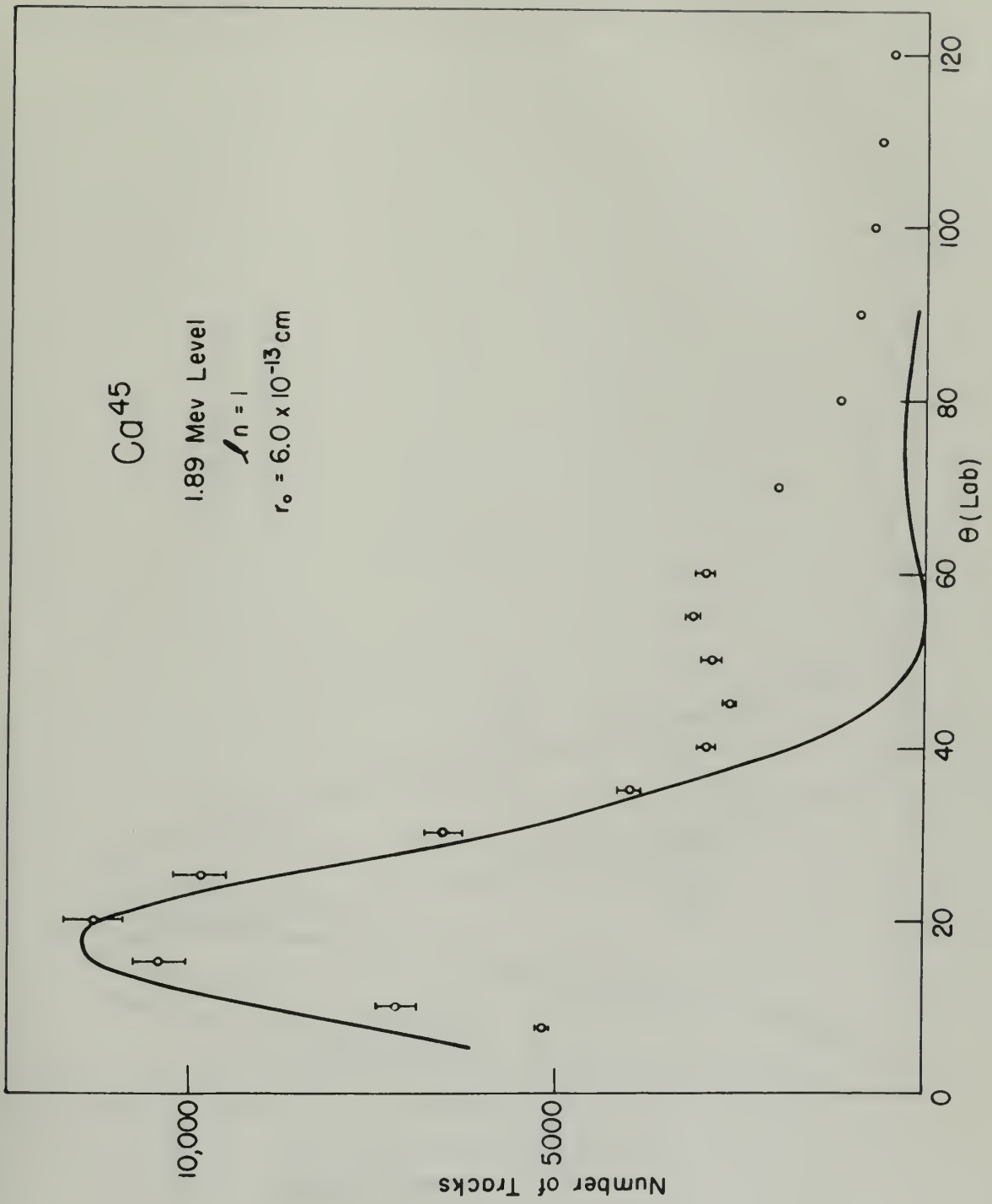


Figure 7





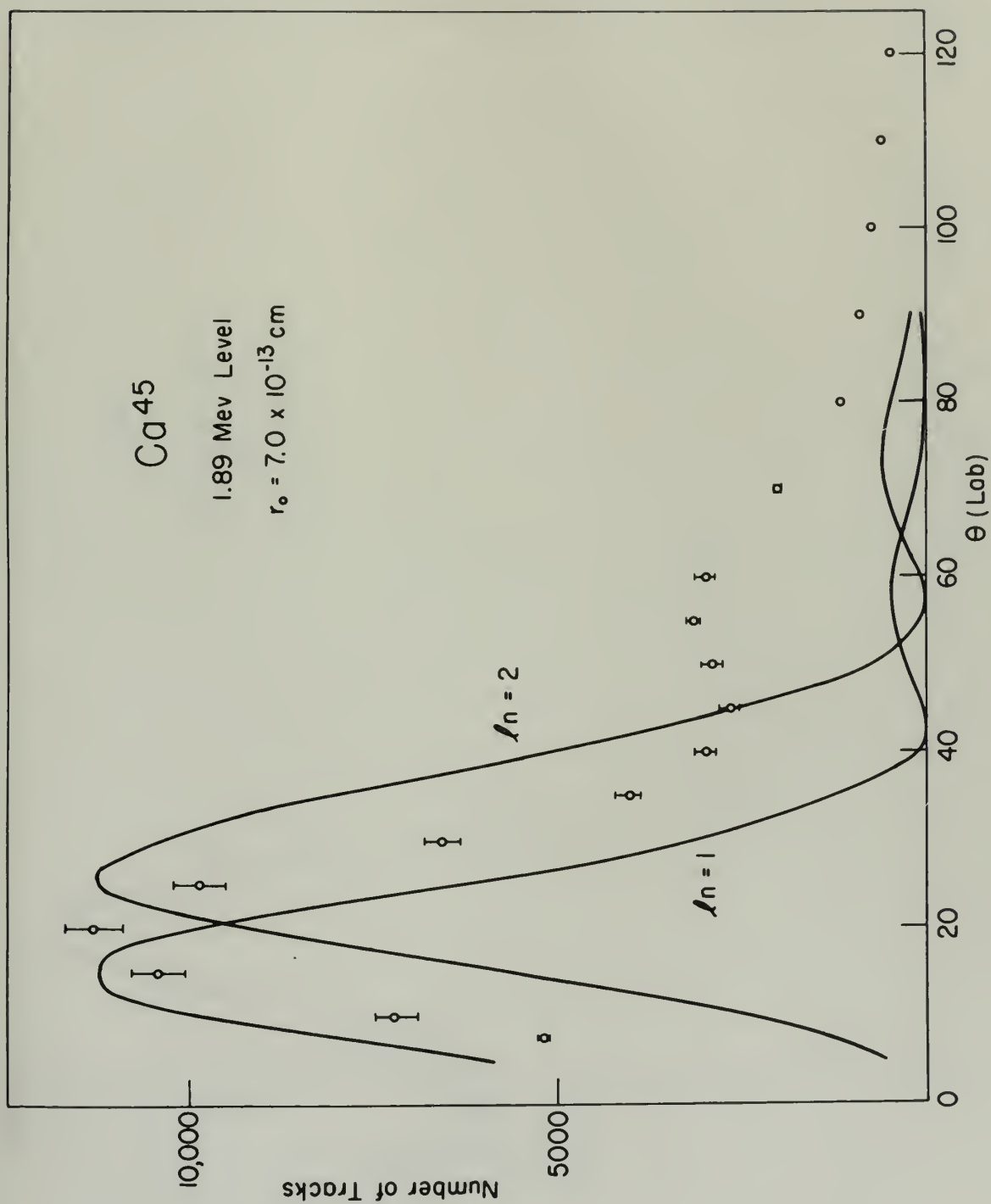


Figure 8



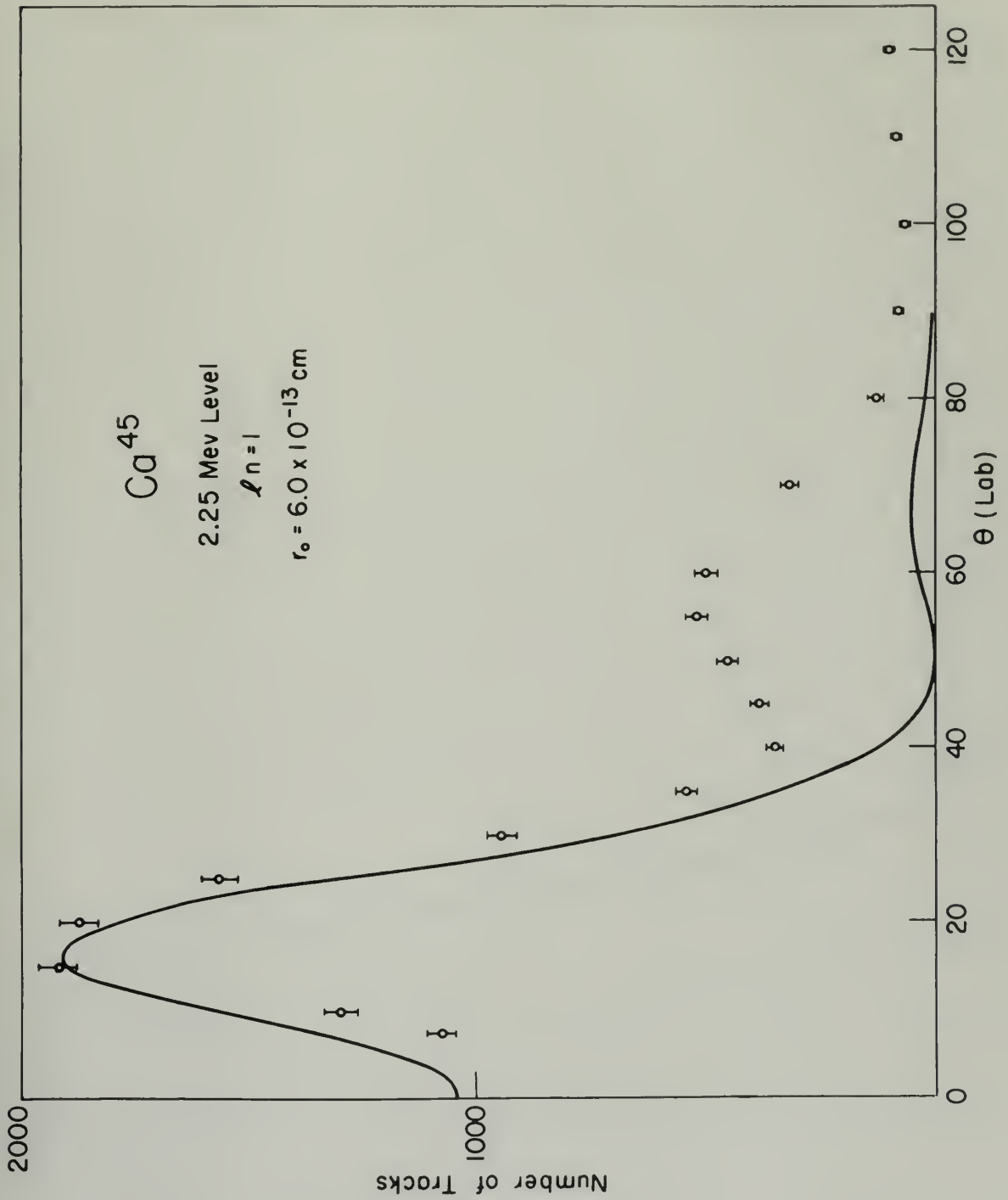


Figure 9





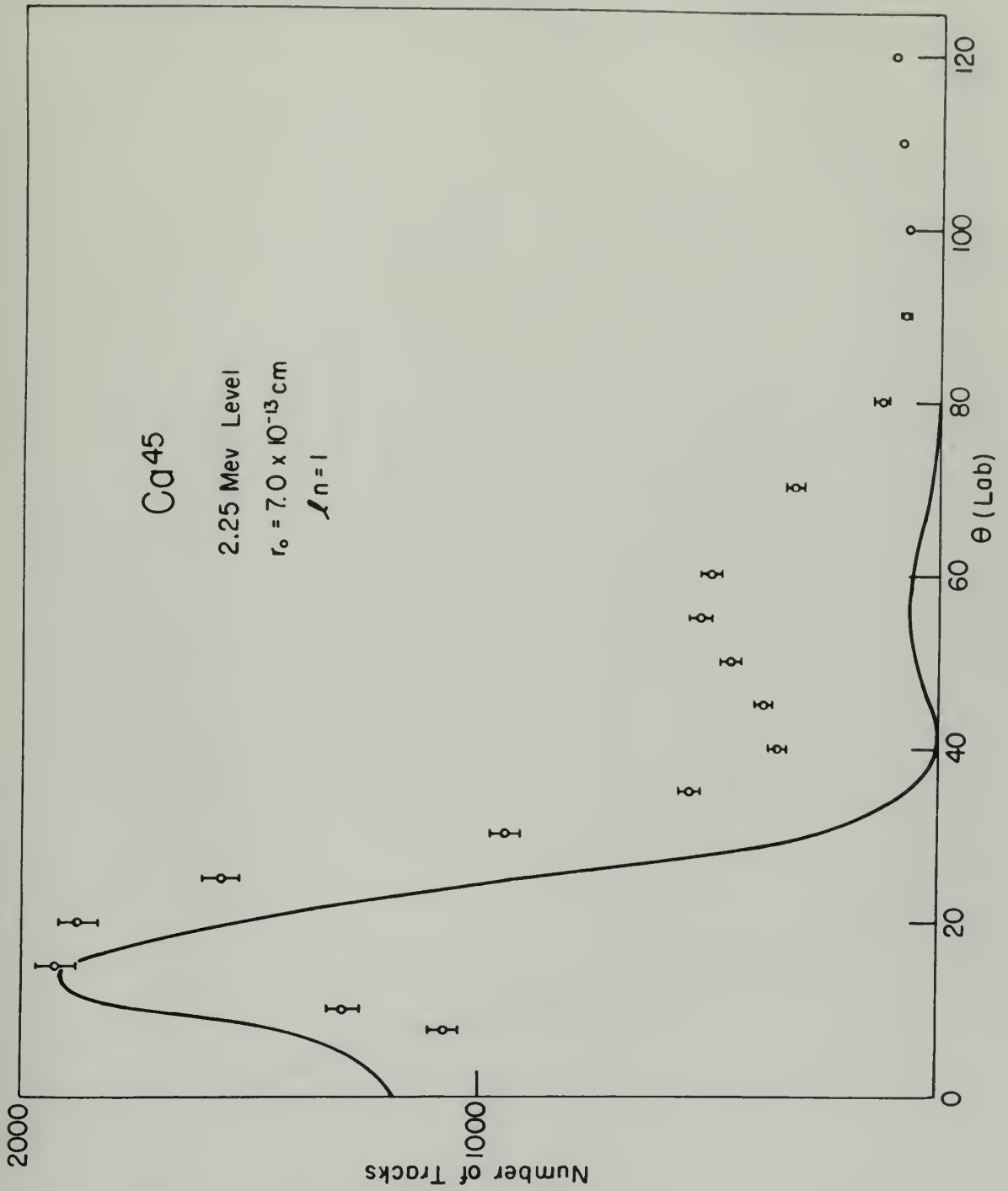


Figure 10



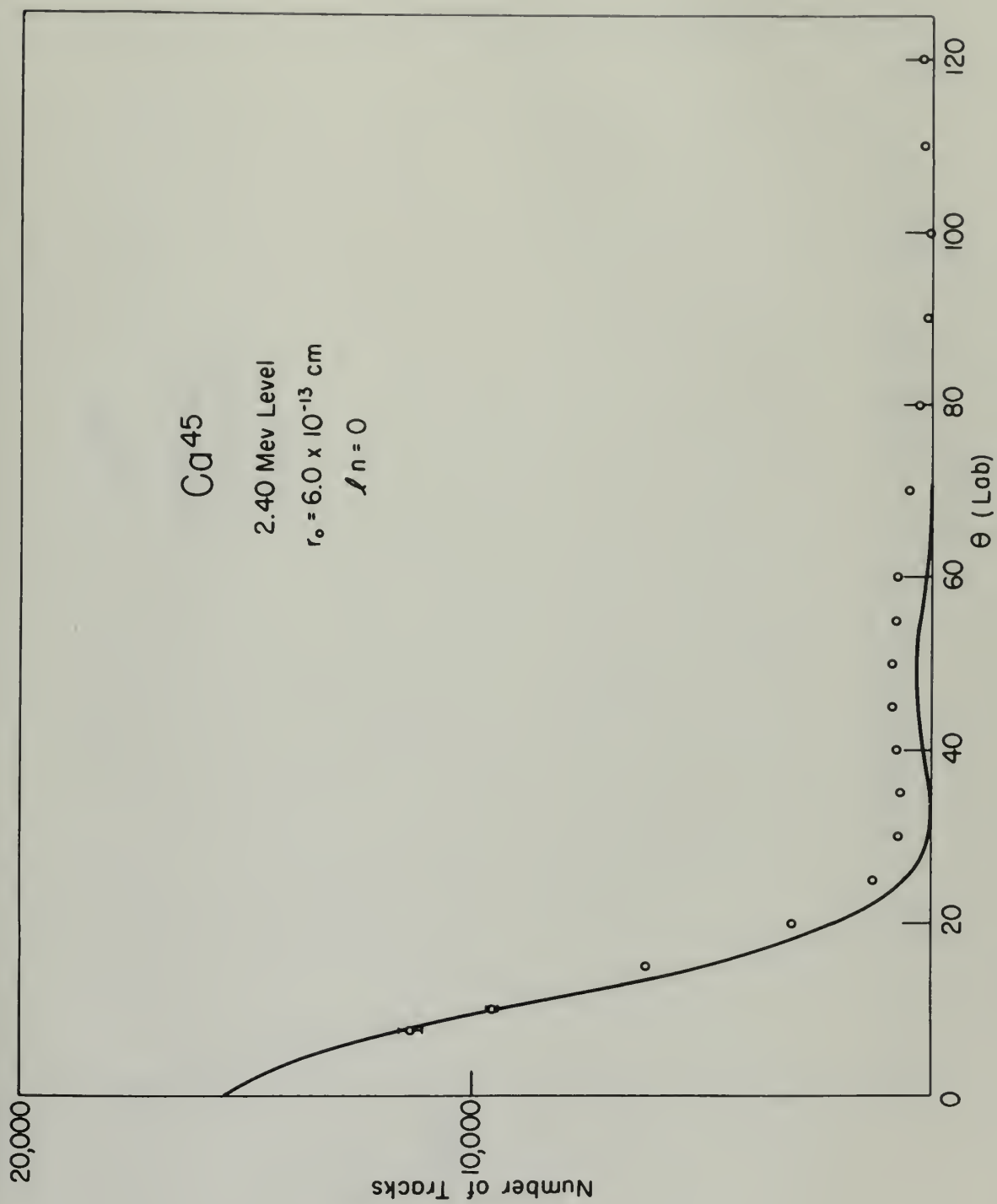


Figure 11





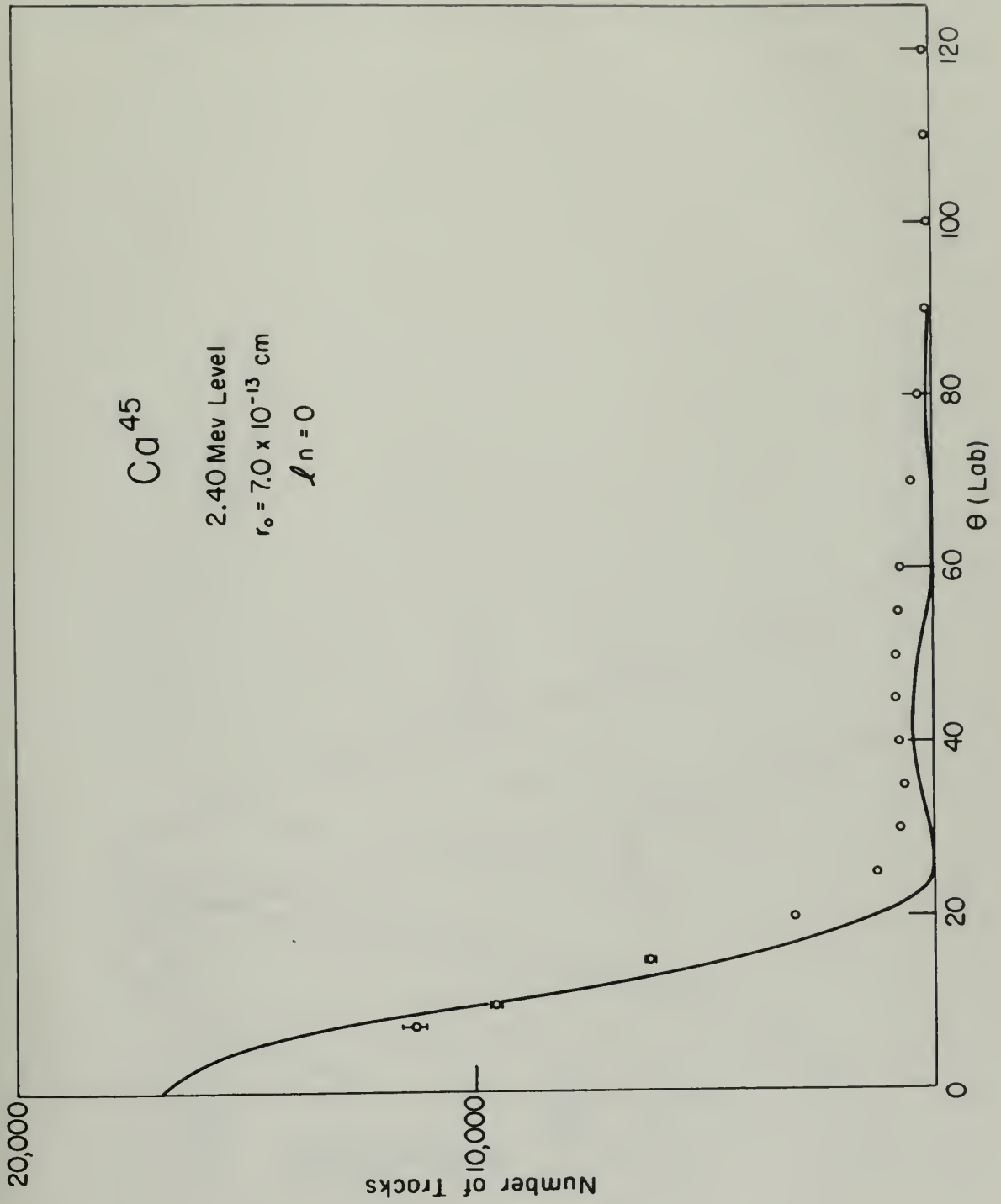


Figure 12



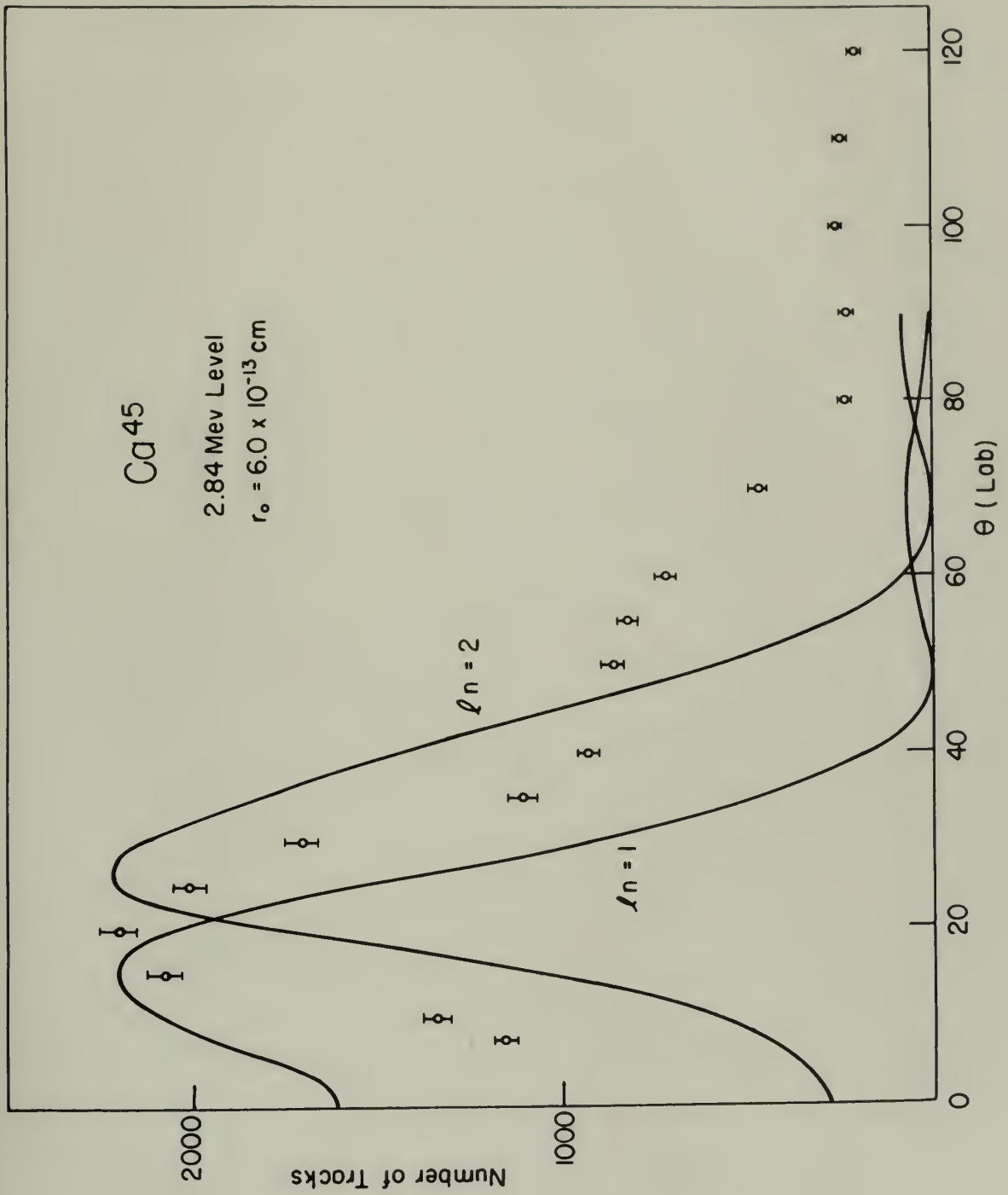


Figure 13



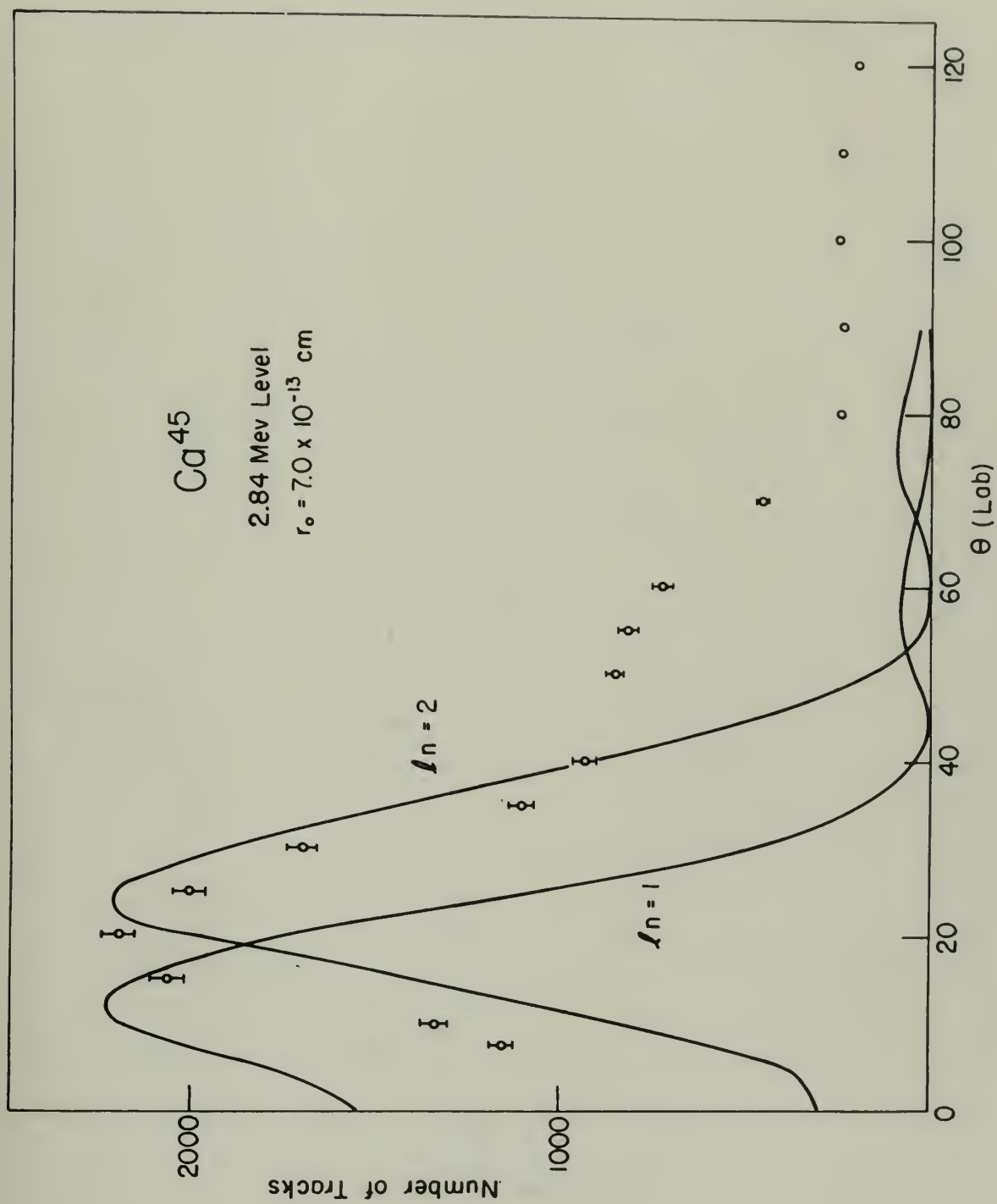


Figure 14





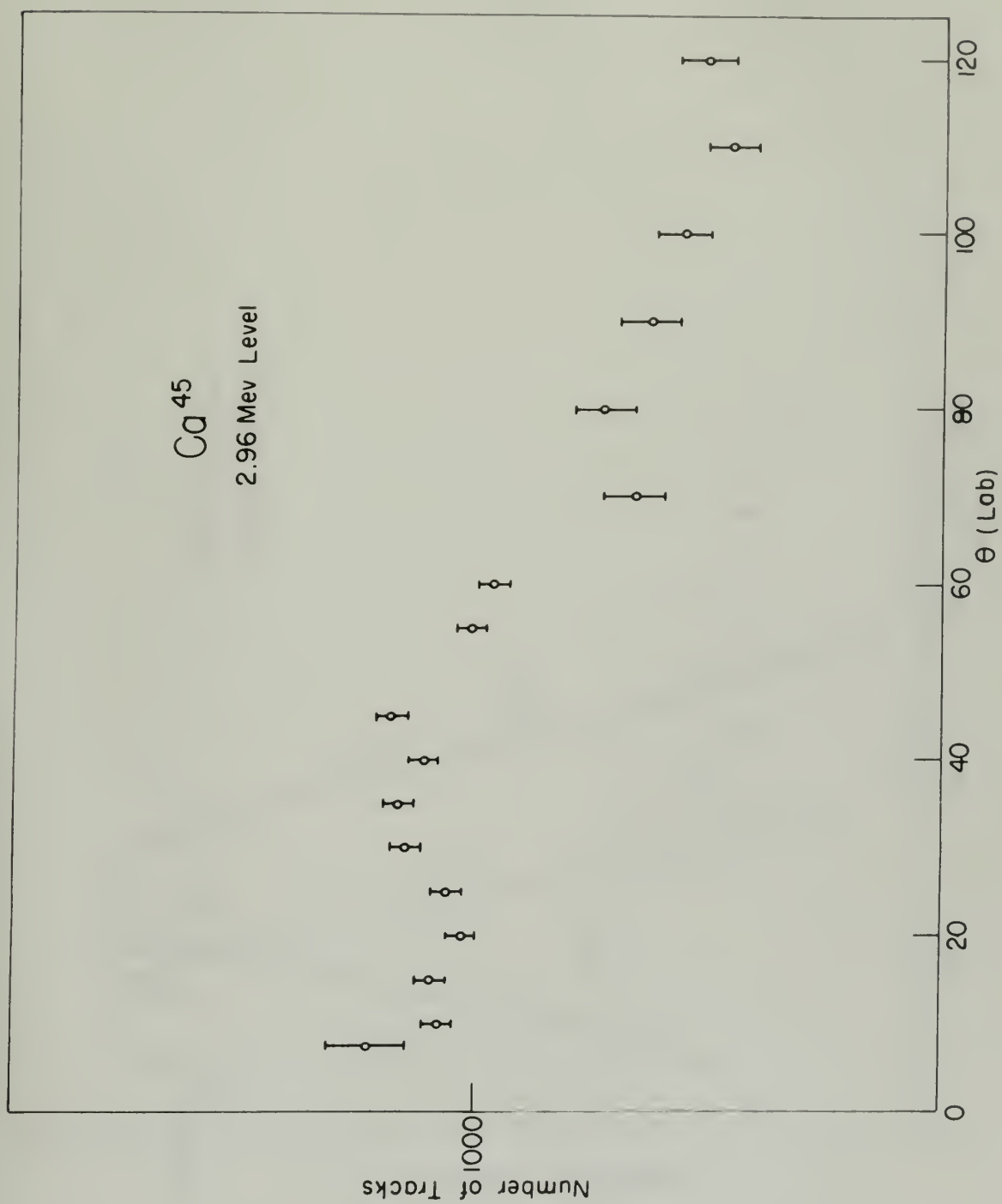


Figure 15



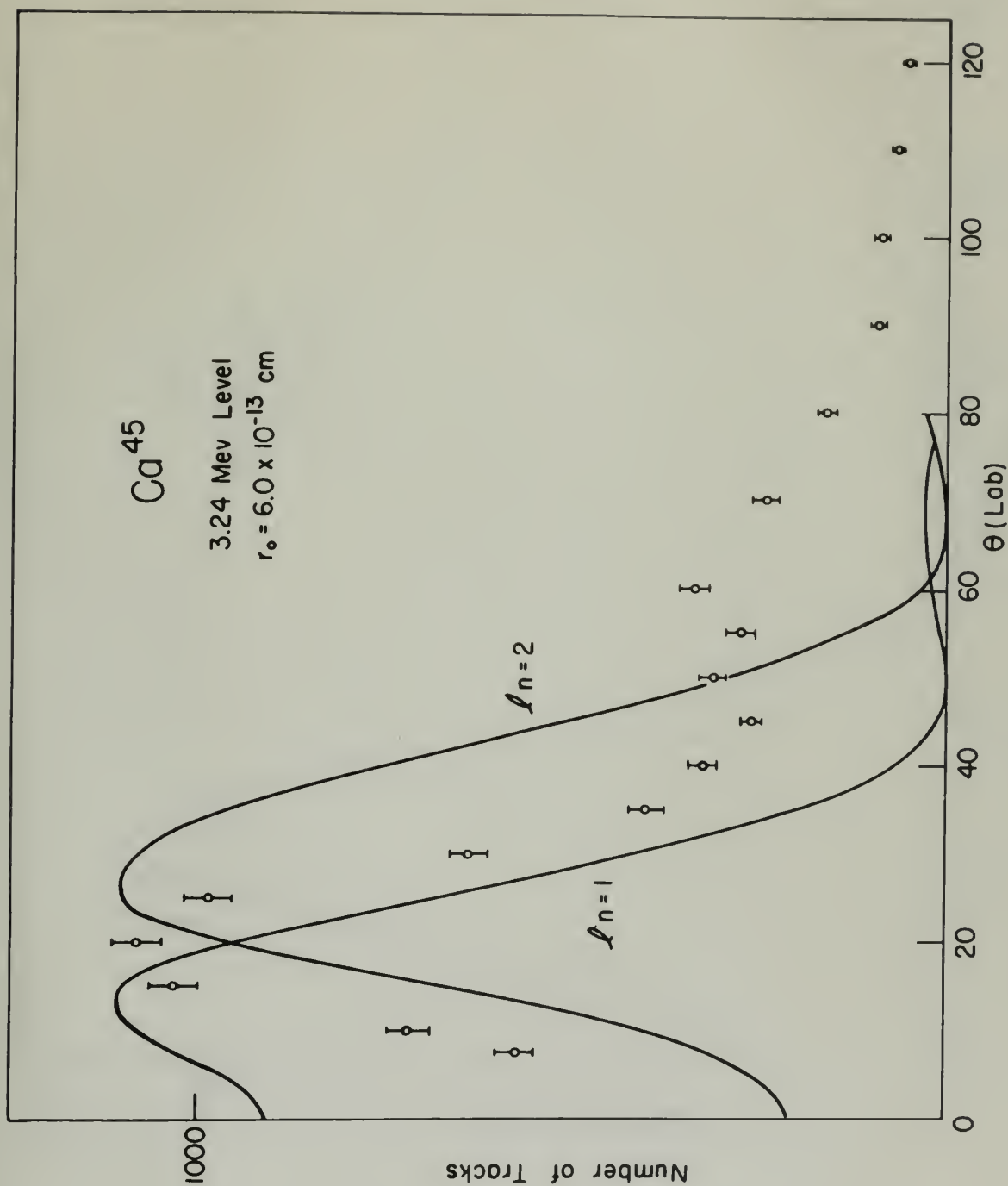


Figure 16





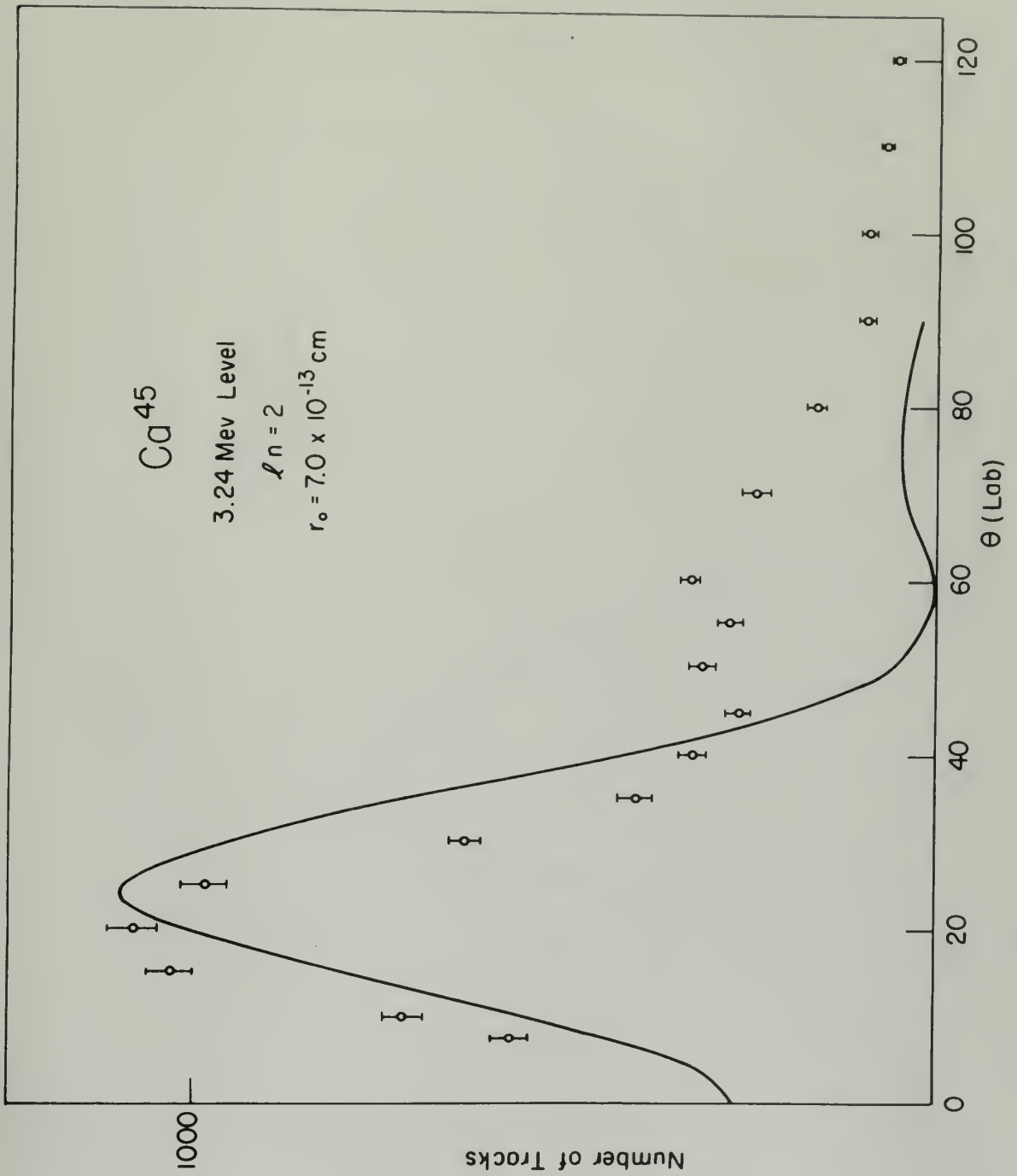


Figure 17



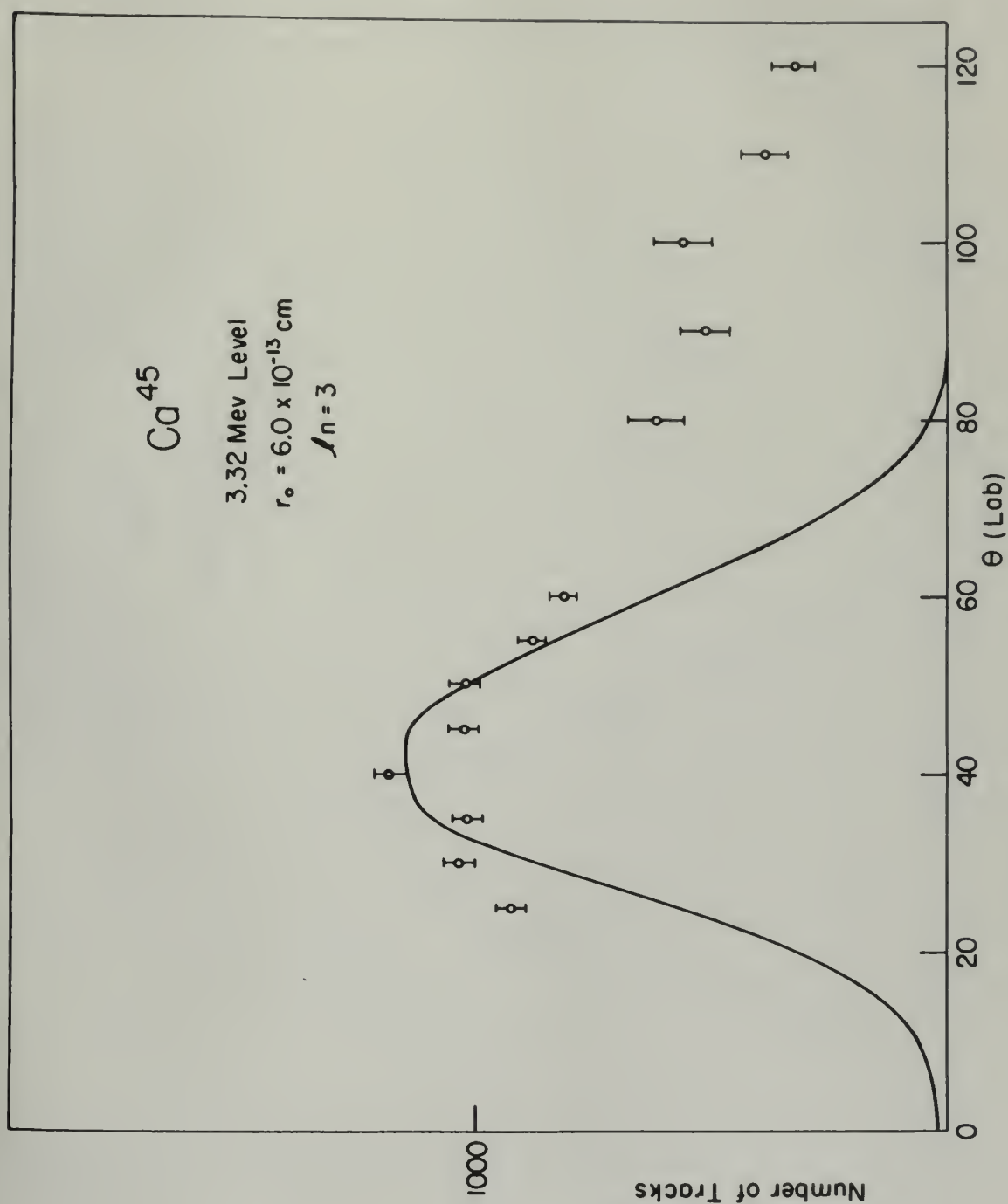


Figure 18



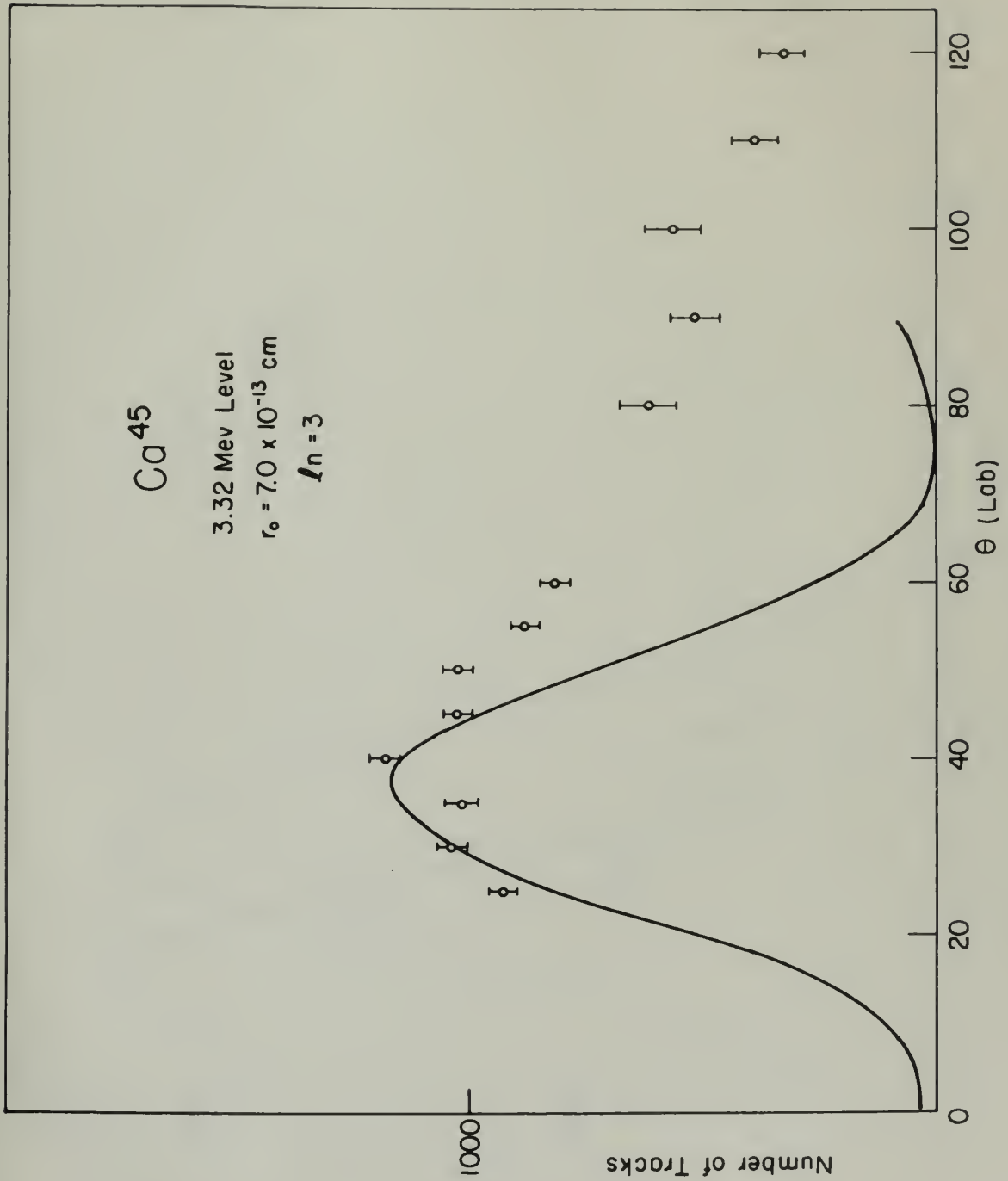


Figure 19





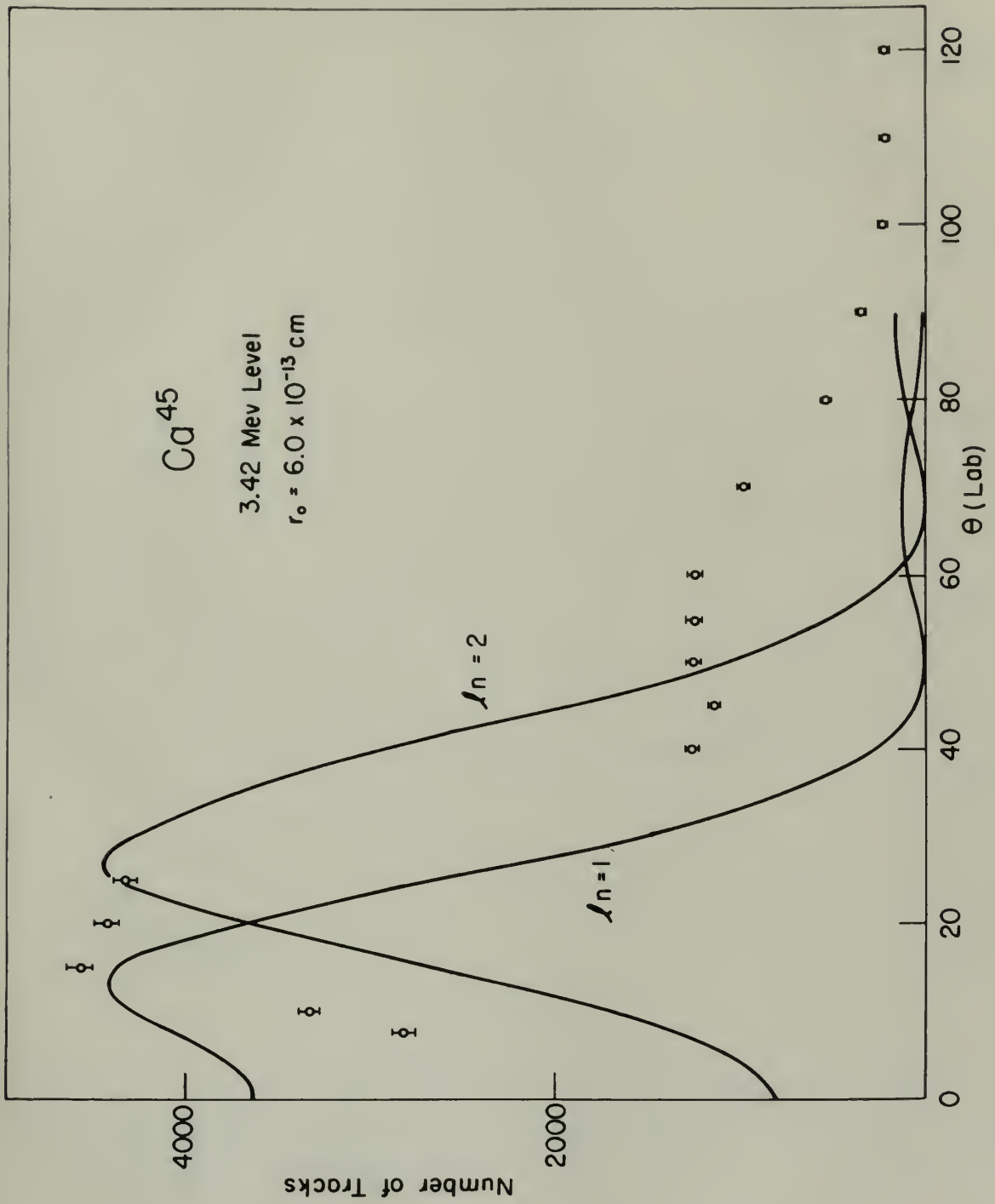


Figure 20



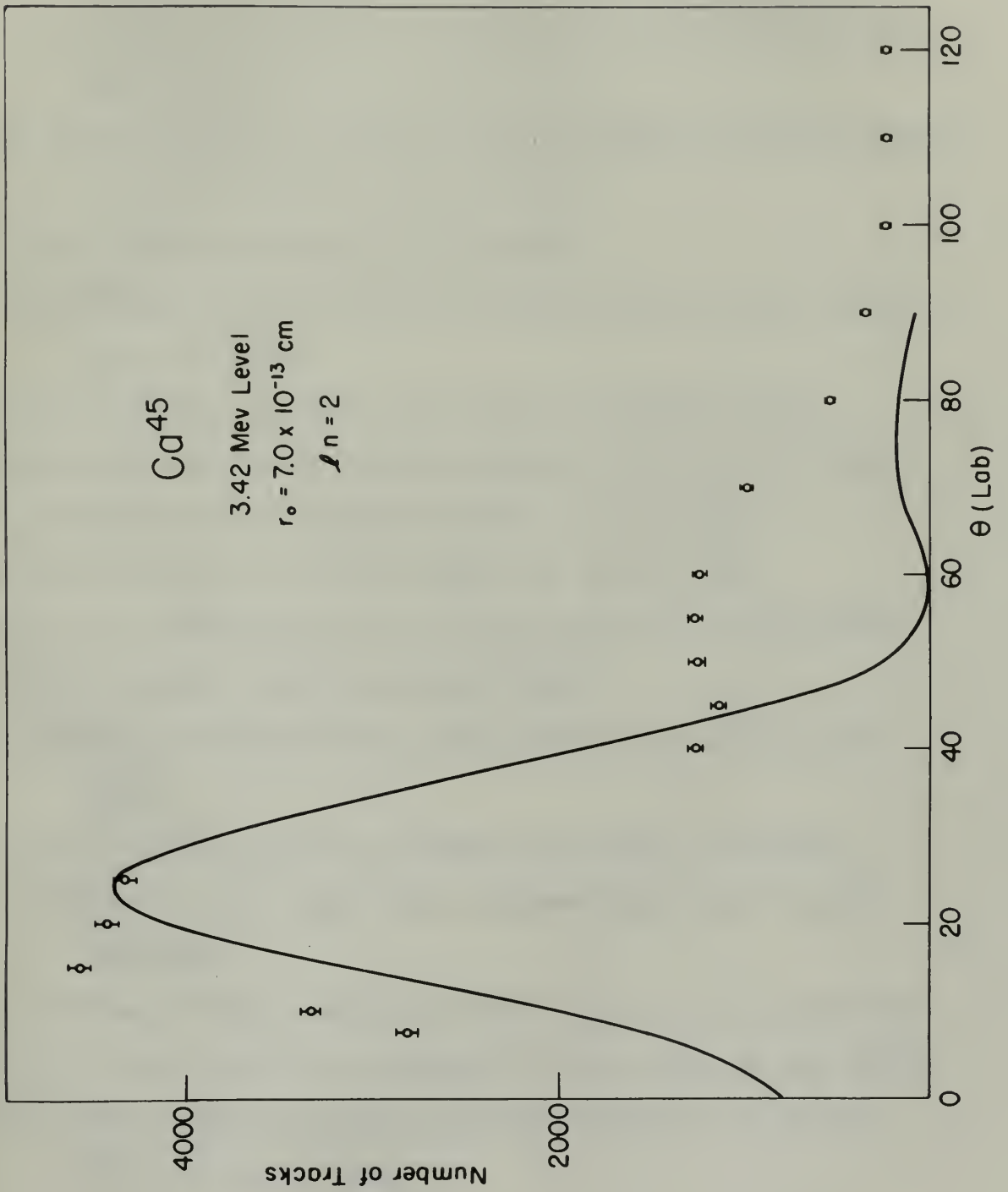


Figure 21





## R E F E R E N C E S

1. D. Kurath, *Phys. Rev.* 91, 1430 (1953).
2. A. R. Edmonds and B. H. Flowers, *Proc. Roy. Soc. (London)*, A215, 120 (1952).
3. Braams, Bockelman, Browne, and Buechner, *Phys. Rev.* 474, 91 (1953).
4. C. M. Braams, *Phys. Rev.* 763, 94 (1954).
5. C. M. Braams, *Phys. Rev.* 95, 650 (1954).
6. Bockelman, Braams, Buechner, and Guthrie, *Bull. Amer. Phys. Soc.* 30, No. 3, 55 (1955).
7. S. T. Butler, *Proc. Roy. Soc. (London)*, A208, 559 (1951).
8. C. M. Braams, *Nuclear Science Abstracts*, Vol. 8, No. 18B (1954).
9. H. Schuler and T. Schmidt, *Naturwiss.* 22, 758 (1934).
10. W. G. Proctor and F. C. Yu, *Phys. Rev.* 81, 20 (1951).
11. C. F. G. Delaney and H. H. J. Poole, *Phys. Rev.* 89, 529 (1953).
12. B. H. Ketelle, *Phys. Rev.* 80, 758 (1950).
13. Buechner, Sperduto, Browne, and Bockelman, *Phys. Rev.* 91, 1502 (1953).
14. G. M. Foglesong and D. G. Foxwell, M.S. Thesis, MIT (1954).
15. Buechner, Browne, Enge, Mazari, and Buntschuh, *Phys. Rev.* 95, 609 (1954).
16. Buechner, Strait, Sperduto, and Malm, *Phys. Rev.* 76, 1543 (1949).
17. C. R. Lubitz and W. C. Parkinson, *Rev. Sci. Inst.* 26, 400 (1955).
18. R. Huby, Progress in Nuclear Physics, edited by O. R. Frisch, Vol. 3, Sect. 7 (1953).

# REFERENCES

1. D. Kurat, *Phys. Rev.* 91, 1130 (1953).
2. A. R. Edwards and R. H. Fingers, *Proc. Roy. Soc. (London)*, A232, 110 (1955).
3. J. J. Thomson, *Proc. Roy. Soc. (London)*, A232, 110 (1955).
4. G. M. Brown, *Phys. Rev.* 103, 91 (1954).
5. G. M. Brown, *Phys. Rev.* 95, 650 (1954).
6. J. J. Thomson, *Proc. Roy. Soc. (London)*, A232, 110 (1955).
7. E. T. Dyer, *Proc. Roy. Soc. (London)*, A232, 110 (1955).
8. G. M. Brown, *Nuclear Science Abstracts*, Vol. 8, No. 122 (1954).
9. H. Schuler and T. Schmidt, *Naturwissenschaften*, 42, 758 (1954).
10. W. G. Proctor and F. G. In, *Phys. Rev.* 81, 30 (1951).
11. C. F. G. Tolmou and H. H. J. Poole, *Phys. Rev.* 80, 523 (1953).
12. R. H. Kestell, *Phys. Rev.* 10, 758 (1950).
13. J. J. Thomson, *Proc. Roy. Soc. (London)*, A232, 110 (1955).
14. G. M. Brown and R. G. Fingers, *Proc. Roy. Soc. (London)*, A232, 110 (1955).
15. J. J. Thomson, *Proc. Roy. Soc. (London)*, A232, 110 (1955).
16. J. J. Thomson, *Proc. Roy. Soc. (London)*, A232, 110 (1955).
17. G. R. Lister and W. G. Fingers, *Proc. Roy. Soc. (London)*, A232, 110 (1955).
18. R. Lister, *Proc. Roy. Soc. (London)*, A232, 110 (1955).

19. G. Gamow and C. L. Critchfield, Theory of Atomic Nucleus and Nuclear Energy Sources, Clarendon Press, Oxford (1950).
20. W. Toboeman, Phys. Rev. 94, 1655 (1954).
21. W. Toboeman and M. H. Kalos, Phys. Rev. 97, 132 (1955).

19. G. Gandy and C. I. Oxtcliffe, Theory of Atomic Systems and

Nuclear Energy Levels, Clarendon Press, Oxford (1950).

20. W. Tobochnik, Phys. Rev. 91, 1652 (1952).

21. W. Tobochnik and W. R. Kates, Phys. Rev. 91, 132 (1952).

22. W. R. Kates, Phys. Rev. 91, 132 (1952).

23. W. R. Kates, Phys. Rev. 91, 132 (1952).

24. W. R. Kates, Phys. Rev. 91, 132 (1952).

25. W. R. Kates, Phys. Rev. 91, 132 (1952).

26. W. R. Kates, Phys. Rev. 91, 132 (1952).

27. W. R. Kates, Phys. Rev. 91, 132 (1952).

28. W. R. Kates, Phys. Rev. 91, 132 (1952).

29. W. R. Kates, Phys. Rev. 91, 132 (1952).

30. W. R. Kates, Phys. Rev. 91, 132 (1952).

31. W. R. Kates, Phys. Rev. 91, 132 (1952).

32. W. R. Kates, Phys. Rev. 91, 132 (1952).

33. W. R. Kates, Phys. Rev. 91, 132 (1952).

34. W. R. Kates, Phys. Rev. 91, 132 (1952).

35. W. R. Kates, Phys. Rev. 91, 132 (1952).

36. W. R. Kates, Phys. Rev. 91, 132 (1952).

37. W. R. Kates, Phys. Rev. 91, 132 (1952).

38. W. R. Kates, Phys. Rev. 91, 132 (1952).

39. W. R. Kates, Phys. Rev. 91, 132 (1952).

40. W. R. Kates, Phys. Rev. 91, 132 (1952).











Thesis  
C528

28913

Cobb  
Angular distribution  
on protons ...

Thesis  
C528

28913

Cobb  
Angular distribution on  
protons ...

thesC528

Angular distribution of protons from Ca



3 2768 002 09443 5

DUDLEY KNOX LIBRARY